

# Petrogenetic and Metallogenetic Relationships in the Eastern Cordillera Occidental of Central Peru



Thomas Bissig and Richard M. Tosdal

Department of Earth and Ocean Sciences, Mineral Deposit Research Unit, University of British Columbia,  
6339 Stores Road, Vancouver, British Columbia V6T 1Z4, Canada  
(e-mail: tbissig@eos.ubc.ca)

## ABSTRACT

Ore deposits spatially and temporally related to high-K calc-alkaline intrusions or domes are widespread in the central Peruvian Cordillera Occidental. Geochronology and petrochemistry of intrusive rocks associated with mineralization reveal that most ore deposits (1) were emplaced in the late Middle to early late Miocene and (2) are related to calc-alkaline igneous rocks of granodioritic composition with  $Sm/Yb > 3$ ,  $Sr/Y > 40$ , and  $Y/Th < 1.5$ . The largest deposits are associated with intrusions with  $Sm/Yb > 4$ . Strontium isotopic compositions of the igneous rocks vary from  $^{87}Sr/^{86}Sr = 0.7038$  to  $0.7089$ , but the  $^{87}Sr/^{86}Sr$  ratio values exhibit only a poorly defined overall trend toward increased crustal contamination through time. Lead isotopic ratios generally correlate with the Sr isotopes and range from  $^{206}Pb/^{204}Pb = 18.64$  to  $18.91$ , from  $^{207}Pb/^{204}Pb = 15.58$  to  $15.66$ , and from  $^{208}Pb/^{204}Pb = 38.60$  to  $39.06$ . The overall Sr and Pb isotopic compositions of the igneous rocks indicate a generally moderate crustal assimilation of ancient radiogenic rocks. The Pb isotopic composition of sulfides from 14 polymetallic ore deposits in the study area lie on parallel arrays between the Pb isotopic compositions of spatially related igneous rocks and higher  $^{208}Pb/^{204}Pb$  and  $^{207}Pb/^{204}Pb$  sources such as Paleozoic and Mesozoic siliciclastic sedimentary rocks or the Carboniferous and older crystalline basement. The trace element and radiogenic isotope signature of igneous rocks related to mineralization indicates that these rocks have undergone limited midcrustal and shallow crustal assimilation and reflect melt equilibration in the lower crust at a crustal thickness of more than 40–45 km under conditions where hornblende and garnet were stable in the basaltic lower crustal residuum. Mineralization was favored by a change from normal to flat subduction, resulting in crustal thickening as well as broadening and subsequent cessation of the magmatic arc. However, some igneous rocks apparently unrelated to mineralization have high  $Sm/Yb$  and  $Sr/Y$  ratios as well. Petrographic and Pb isotopic evidence indicates that for some of these rocks, these trace element ratios may be better explained by shallow crustal hornblende fractionation or assimilation of pelitic material.

**Online enhancements:** appendix tables, tab-delimited ASCII data file, Excel data file.

## Introduction

Intrusion-related ore deposits are widespread in the central Peruvian Cordillera Occidental and adjacent high plains to the east (figs. 1, 2). These deposits, while emplaced in shallow crustal environments, are spatially and temporally related to calc-alkaline granitoid intrusions or domes. However, the region also hosts many intrusions with no apparent relationship to significant base and precious metal mineralization. Thus, finding ways to distinguish igneous rocks potentially associated

with mineralization from barren rocks is of importance for regional exploration programs.

The geodynamic environment (i.e., the subduction geometry and subduction of aseismic ridges) greatly influences the generation of potentially fertile versus barren magmas, and changes in subduction parameters are reflected in systematic variations in style and composition of magmatism through time (e.g., Kay et al. 1999; Haschke et al. 2002a, 2002b; Hollings et al. 2005). In central Peru, data on the geochemical evolution of the Neogene magmatic arc are still scarce. However, Bissig et al. (2008) have shown that Neogene magmatism is widespread in the study region but polymetallic

Manuscript received November 3, 2008; accepted March 19, 2009.

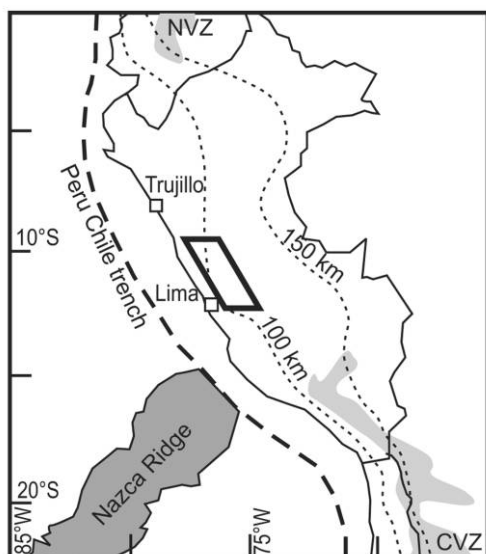


**Figure 1.** Map of Peru showing the outline of the area studied and major plate tectonic features. Small-dashed lines are depth contours of the Wadati-Benioff zone. Light gray areas indicate the approximate extent of volcanic zones (CVZ, Central Volcanic Zone; NVZ, Northern Volcanic Zone). Modified from Gutscher et al. (1999).

mineralization was mostly emplaced in the late middle and late Miocene. In this contribution we present 69 new whole-rock analyses of intrusive and volcanic rocks collected between Antamina (lat 9°32'S) and the Huacravilca intrusion (lat 12°20'S), some 30 km south of Yauricocha (fig. 2). We discuss the petrochemical characteristics of intrusions associated with mineralization of magmatic-hydrothermal origin and compare them with apparently barren intrusions. We also present new radiogenic Pb and Sr isotope data of plagioclase separates from nine unaltered igneous rocks that complement the whole-rock geochemical and published isotope data. New and published (Gunnesch et al. 1990; Beuchat 2003) Pb isotope data of ore minerals from different deposits allow evaluation of the origin of polymetallic mineralization and its relationship to Cenozoic igneous rocks.

### Geological Setting

Eocene to Miocene intrusions and isolated volcanic rocks are emplaced in the Cordillera Occidental and adjacent areas up to 70 km east of this continental divide (Bissig et al. 2008; fig. 2). The rocks hosting these intrusions consist of a wide spectrum of marine and continental sedimentary rocks, as well as subordinate volcanic and intrusive rocks

ranging from Paleozoic to Paleogene in age (Benavides 1999). The Mesozoic was dominated by a Mariana-type subduction system, with the mainly shallow marine and siliciclastic sedimentary sequences being deposited in a back-arc setting (Benavides 1999) that persisted until the Aptian in the study region (Bissig et al. 2008), after which the opening of the south Atlantic led to a more compressional regime and cessation of back-arc spreading (Mochica tectonic phase; Mégard 1984). Magmatism in the Upper Cretaceous is represented by the 100–60-Ma Coastal Batholith (Cobbing 1973) and farther east in the study area by 77-Ma calc-alkaline basaltic rocks (Bissig et al. 2008) intruding the Upper Cretaceous Casapalca Formation red beds.

The Mesozoic shallow marine and siliciclastic sedimentary rocks were intensely folded during the Paleocene to Eocene Incaic Orogenic phase and are included in the Marañón fold-and-thrust belt (Benavides 1999). Subsequent contractile deformation up to the middle to late Miocene has been documented in the study area (Farrar and Noble 1976).

### The Ore Deposits of Central Peru

The central Peruvian cordillera is host to a wide variety of magmatic-hydrothermal ore deposits. Mineralization styles range from Cu-Zn (Mo-) skarn at Antamina (Love et al. 2004) to shallow cordilleran base metal lode and high-sulfidation Au-Ag replacement deposits (e.g., Colquijirca and Cerro de Pasco; Bendezú et al. 2004, 2008; Vidal and Ligarda 2004; Baumgartner et al. 2008). Silver-rich polymetallic vein deposits include the Uchucchacua (Bussell et al. 1990; Petersen et al. 2004) and San Cristóbal (Beuchat et al. 2004) vein systems, whereas high-sulfidation epithermal precious metal mineralization hosted by volcanic rocks is known from the Carhuacayán and Quicay deposits (table A1, available in the online edition or from the *Journal of Geology* office). All of these deposits are related to igneous rocks. For most it can be readily discerned which of the intrusive rocks are genetically (e.g., if endoskarn is present) or at least spatially and temporally related to the mineralization. At only a few deposits, no igneous rocks potentially related to the mineralization have been recognized; a syngenetic or diagenetic origin has been proposed for some (e.g., Cercapuquio; Cedillo and Tejada 1988).

The ore deposits were generally emplaced in the middle and late Miocene. Arc volcanism decreased and finally ceased in the late Miocene, likely be-

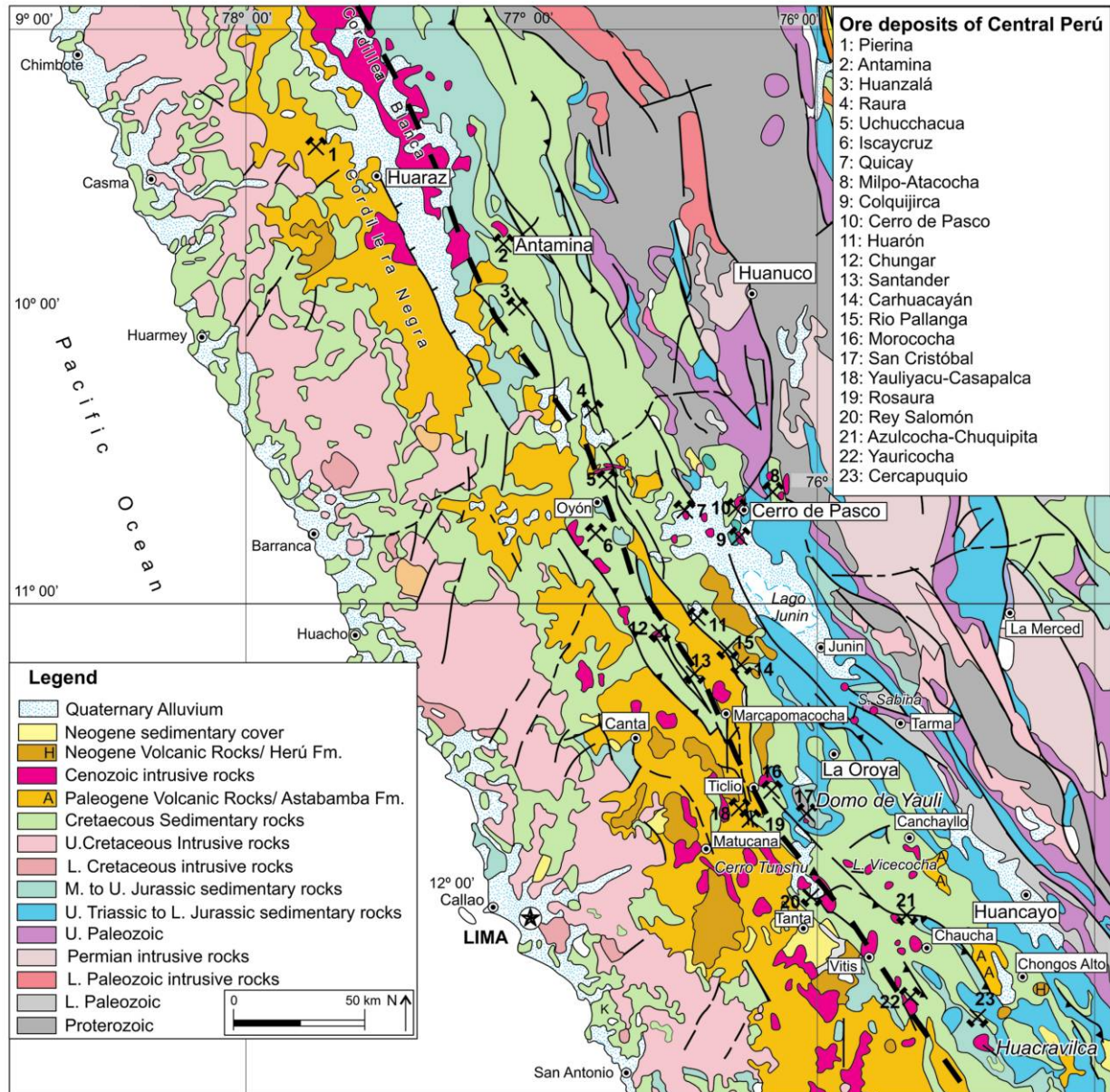


**Figure 2.** Geological map of central Peru (modified from Instituto Geológico Minero y Metalúrgico 1995; some Cenozoic intrusions have been added). The dashed line delineates the continental divide represented by the Cordillera Occidental. The extent of the Paleogene volcanic rocks roughly corresponds to the extent of the Calipuy Supergroup as mapped in central Peru. Paleogene volcanic rocks west and south of Huancayo correspond to the Astabamba Formation (A), whereas Neogene rocks correspond to the Herú Formation (H). The ore deposits and locations mentioned in the text are indicated.

cause of slab flattening related to the subduction of the aseismic Nazca ridge (Noble and McKee 1999; Hampel 2002; Rosenbaum et al. 2005; Bissig et al. 2008). However, some Eocene and Oligocene ore deposits occur in a broad east-west transect from Uchucchacua to Milpo (Bissig et al. 2008). The giant middle and late Miocene cordilleran base

metal deposits of Colquijirca and Cerro de Pasco are contained within this transect as well, and Bissig et al. (2008) suggest an important lineament control on the distribution of these deposits across the strike of the Andes (cross-strike discontinuity; Love et al. 2004).

The principal characteristics and ages of the ore

deposits within the study area are summarized in table A1. For a further comprehensive collection of references, see Noble and McKee (1999) and Rosenbaum et al. (2005).

### The Petrochemical Evolution of the Central Peruvian Intrusions

**Data and Analytical Methods.** Our database includes 69 whole-rock analyses of igneous rocks representing mostly Eocene to late Miocene intrusions and volcanic rocks. This database has been complemented by seven compiled analyses from the Domo de Yauli area (lat 11°40'S, long 76°W; Beuchat 2003) and the Bosque de Piedra ignimbrite (Soler 1991). Igneous rocks were sampled and analyzed for major elements by lithium metaborate fusion and inductively coupled plasma-atomic emission spectroscopy, whereas trace elements were determined by lithium borate fusion and inductively coupled plasma-mass spectroscopy (ICP-MS) at the ALS Chemex laboratories in North Vancouver, Canada. Some trace elements, including rare earth elements (REEs) and Y, have been analyzed by HF/HNO<sub>3</sub> solution ICP-MS (see Jenner et al. 1990) at Memorial University at St. John's, Newfoundland, Canada. Seven samples of igneous rocks from south of Domo de Yauli, plus one from Antamina and one from Carhuacayán, have been chosen for <sup>87</sup>Sr/<sup>86</sup>Sr and Pb isotopic analyses carried out at the Pacific Centre for Isotope research at the University of British Columbia in Vancouver. The isotopic analyses, with exception of one whole-rock analysis (2PYB524), were performed on mineral separates of unaltered plagioclase. The Pb isotopic composition was additionally determined for 24 sulfide samples from 10 different ore deposits in central Peru. Pb isotopes were measured on a multicollector ICP-MS system, whereas Sr isotopic analyses were carried out on a Finnigan TRITON thermal ionization mass spectrometer. The standards used were NBS 987 for Sr and NBS 981 for Pb isotopes (for details on analytical methods, see Weis et al. 2005, 2006). The analytical data are available in tables A2–A4, available in the online edition or from the *Journal of Geology* office, and in a data file, available as an Excel file or as a tab-delimited ASCII file. Reliable age constraints are available for the majority of the analyzed rocks and are, unless indicated otherwise, from Bissig et al. (2008).

**Eocene Magmatism and Mineralization.** Eocene intrusions ranging in age from 49 to 33 Ma occur in a variety of locations, including a ~40-Ma intrusion along the access road to Antamina (D. Love, 2003, pers. comm.) and 33.5- to 37.5-Ma dacitic

domes west of Cerro de Pasco. At the southern end of the study area, Eocene intrusions include the 39.34 ± 0.28-Ma granodioritic Huacravilca intrusion (fig. 2) and a coarsely porphyritic rhyolite dike (40.14 ± 0.61 Ma) near Canchayllo, as well as 36.1–33.1-Ma hornblende phyric diorite bodies west of Chaucha (and north of Yauricocha; fig. 2). All of these rocks are subalkaline, belong to the high-K calc-alkaline series, and range from andesitic to dacitic compositions (fig. 3A, 3B). In most samples, the light rare earth elements (LREEs) are enriched, whereas the heavy rare earth elements (HREEs) have relatively flat patterns in the chondrite-normalized REE plots (fig. 3C, 3D). However, the intrusions west of Chaucha are distinct in that they have variable and in some samples strongly fractionated HREE patterns (fig. 3E) with Sm/Yb values ranging from 2.4 to 10, the highest ratio from a hornblende and plagioclase porphyritic dike. This dike crops out near a large but petrographically similar diorite intrusion at Chaucha and is most likely related to it. These same intrusions also have more variable Sr contents (379–867 ppm) than the other Eocene igneous rocks. The wide range in Sm/Yb ratios and Sr content in these intrusions is interpreted as the result of fractional crystallization of hornblende, plagioclase, and accessory phases during ascent and emplacement of these magmas.

Eu/Eu\* values in Eocene rocks are generally minor, between 0.8 and 1 (fig. 3F), except for rhyolite sample PCB600, which has a Eu/Eu\* value of 0.62. Considering the low to moderate Sr concentrations (323–551 ppm) of Eocene rocks (excluding the Chaucha area intrusions), we suggest that some plagioclase fractionation probably occurred but that the magmas were generally oxidized. None of the Eocene rocks analyzed is related to significant polymetallic mineralization, but Eocene mineralization is known from the 37.5-Ma (Noble and McKee 1999) Quicay high-sulfidation epithermal system, located west of Cerro de Pasco (fig. 2, 7).

**Early Oligocene Magmatism and Mineralization.** A number of mostly small early Oligocene dioritic to granodioritic porphyry stocks intruded at Milpo and near Ticlio (fig. 2). Relatively voluminous early Oligocene extrusive volcanism is manifested in the 32–31-Ma andesitic to dacitic Astabamba Formation (fig. 2), in the southeastern part of the study area. Important Pb-Zn skarn mineralization was emplaced at approximately 29.3 Ma at Milpo and is associated with potassium-feldspar-altered dacitic porphyry lacking phenocrystic quartz (Milpo stock; fig. 2, 8). Numerous other quartz-phyric, dacite porphyry stocks of the area of similar to slightly older age (Soler and Bonhomme 1988;

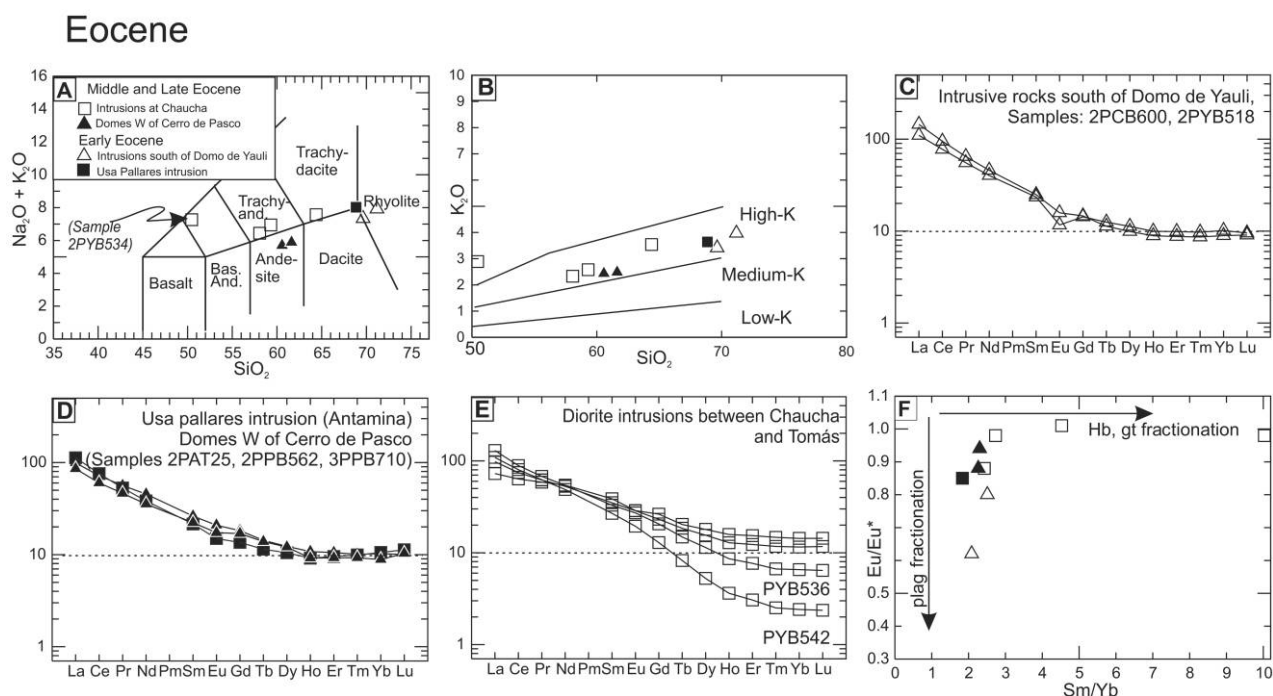


**Figure 3.** General geochemical characteristics of Eocene intrusive and volcanic rocks. *A*, Total alkali versus silica diagram from LeBas et al. (1986). The samples straddle the border between alkaline and calc-alkaline series. Sample PYB534 has experienced minor hydrothermal alteration. Note that for simplicity, fields are labeled using the terms for volcanic rocks only, but data include volcanic and intrusive rocks. *B*,  $K_2O$  versus silica diagram after Peccerillo and Taylor (1976). All rocks are high-K calc-alkaline, but the intrusions at Chaucha have generally slightly elevated K contents compared with those of the other samples. *C–E*, Chondrite-normalized spider diagrams for rare earth elements. Normalization values from Sun and McDonough (1989). *F*, Europium anomaly ( $Eu/Eu^*$ ) versus Sm/Yb ratios as a proxy for plagioclase (*plag*) versus garnet (*gt*) and/or hornblende (*hb*) fractionation. No clear overall fractionation trend is evident.

Bissig et al. 2008) are unrelated to polymetallic mineralization.

As in the Eocene, early Oligocene magmatism was high-K calc-alkaline. The intrusions at Ticlio and Milpo have high potassium contents (up to 11.3%  $K_2O$  for the Milpo stock) that, on the basis of petrographic observation, can be attributed to potassic alteration (fig. 4A, 4B). The rocks at Milpo and in the Astabamba Formation are enriched in LREE and exhibit flat to moderately fractionated HREE (fig. 4C–4E;  $Sm/Yb = 2.6–3.7$ ). The highest  $Sm/Yb$  value comes from a dacite dome of the Astabamba Formation, whereas the Milpo stock has a  $Sm/Yb$  ratio of 3.38. The two Ticlio samples have  $Sm/Yb$  values of 3.3 and 4.8. This variation, similar to the Eocene diorites of Chaucha, may be attributed to hornblende and accessory phase fractionation. Eu is slightly depleted in the Milpo intrusions ( $Eu/Eu^* = 0.8$ ) but is not anomalous in the other rocks ( $Eu/Eu^* = 0.9–1$ ; fig. 4F). This indicates that the magmas were relatively oxidized but that

at Milpo, minor plagioclase fractionation may have occurred.

**Late Oligocene Magmatism.** Late Oligocene magmatism is restricted in the study region but has been described from the Cordillera Negra to the northwest (Noble et al. 1999; Strusievicz et al. 2000). Volcanic rocks mapped as the Calipuy Formation (Cobbing 1973) in the wider Uchucchacua area were dated at 25 Ma, with similar ages for K-feldspar-altered intrusions in deep parts of the Uchucchacua mine (fig. 2, 5). Crosscutting relationships indicate that the altered intrusions pre-date at least some of the mineralized veins at Uchucchacua, but the genetic relationship of intrusive rocks with mineralization in the district remains inconclusive (Petersen et al. 2004). A small rhyolite dome and two stocks of dacitic composition, dated at 20.5–21 Ma, define an isolated and small magmatic province without mineralization in the triangle between the towns of Junín, Tarma, and La Oroya.

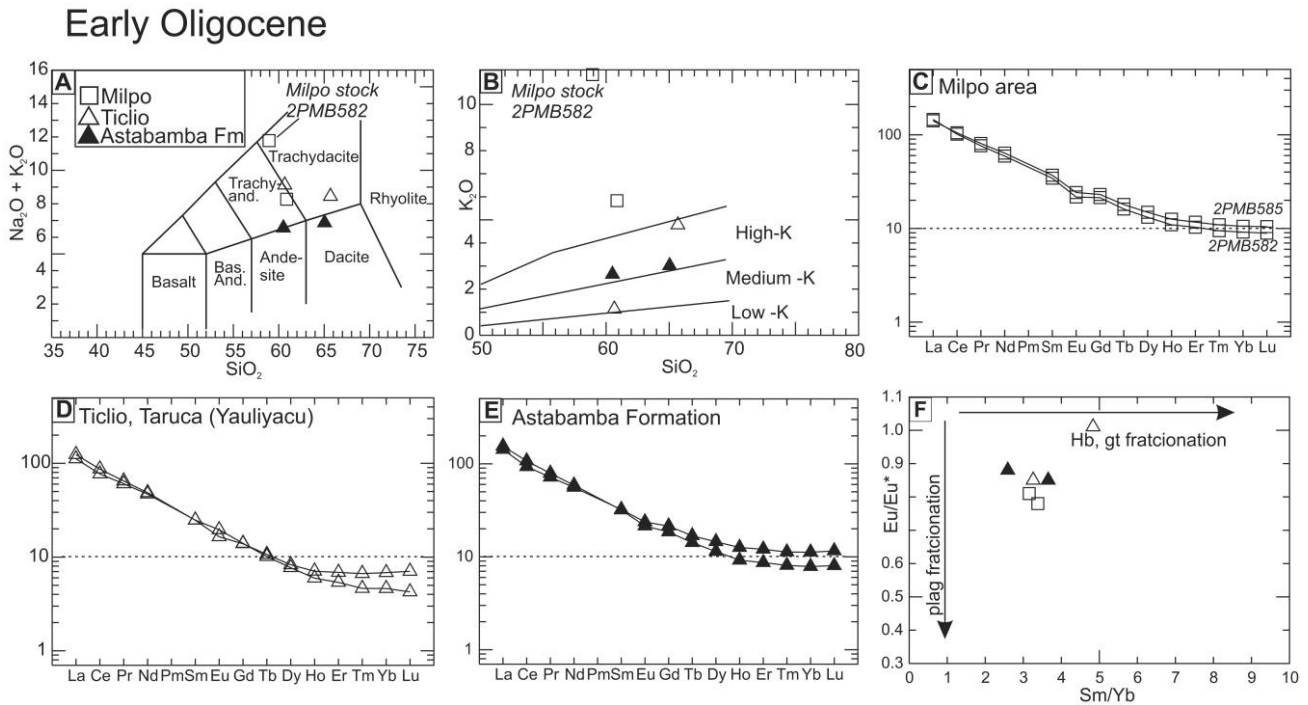


**Figure 4.** General geochemical characteristics of early Oligocene intrusive and volcanic rocks (see fig. 3 for references and abbreviations). *A*, All samples are andesitic to dacitic in composition, but the samples from Milpo, and, to a lesser extent, those from Ticlio, have experienced hydrothermal alteration. *B*, Rocks are high-K calc-alkaline. The sample with the highest potassium content corresponds to the potassically altered Milpo stock. *C–E*, Chondrite-normalized spider diagrams for rare earth elements. *F*, Eu/Eu\* versus Sm/Yb. No clear overall fractionation trend is evident.

All the igneous rocks are of high-K calc-alkaline character; the very-high-K concentrations of the Uchucchacua Oligocene intrusive rocks are related to readily identified K-feldspar alteration (fig. 5A, 5B). HREEs are distinctively more fractionated in the Uchucchacua volcanic rocks ( $Sm/Yb = 4.4–5$ ) than in the younger rocks to the east of La Oroya ( $Sm/Yb = 1.7–3.8$ ; fig. 5C). However, the intrusive rocks possibly associated with mineralization at Uchucchacua exhibit lower  $Sm/Yb$  ratios of 2.97 and 3.36 but HREE concentrations similar to those of the Calipuy group volcanic rocks (fig. 5C). The Eu/Eu\* values of the dacitic rocks are moderate, between 0.7 and 0.9 (fig. 5D). The most anomalous samples are the potassically altered intrusions from the lower parts of the Uchucchacua mine. The Santa Sabina rhyolite dome between La Oroya and Tarma (sample PTB612) has a distinctly deeper Eu anomaly and only 110 ppm Sr, which reflects its rhyolitic composition and indicates extensive feldspar fractionation. South of Domo de Yauli, no Late Oligocene magmatism is known.

#### **Early Miocene Magmatism and Mineralization.**

After the extended magmatic quiescence south of Domo de Yauli, igneous activity resumed at 18.5 Ma with the intrusion of the magmatic garnet-bearing and thus peraluminous rhyolite sill near Canchayllo (fig. 2). This sill and nearby small intrusions exhibit columnar jointing, indicating a shallow level of emplacement. At 17 Ma a voluminous granodioritic to tonalitic complex intruded near Vitis in the Cordillera Occidental west of Yauricocha (fig. 2). The Vitis intrusive phase was followed by small quartz-monzonitic to granitic intrusions (one dated at  $16.2 \pm 0.15$  Ma) approximately 15 km northeast of Vitis. Muñoz (1994) described small-scale skarn mineralization from these intrusions at Chuquipita, but the most significant Zn, Mn, Pb, and Au mineralization was at Azulcocha, also known as Grán Bretaña (fig. 2, 21; Muñoz 1994). The Azulcocha orebody was emplaced in collapse and fault breccias along the Grán Bretaña fault zone, approximately 5 km east of the early Miocene Chuquipita intrusions (Muñoz

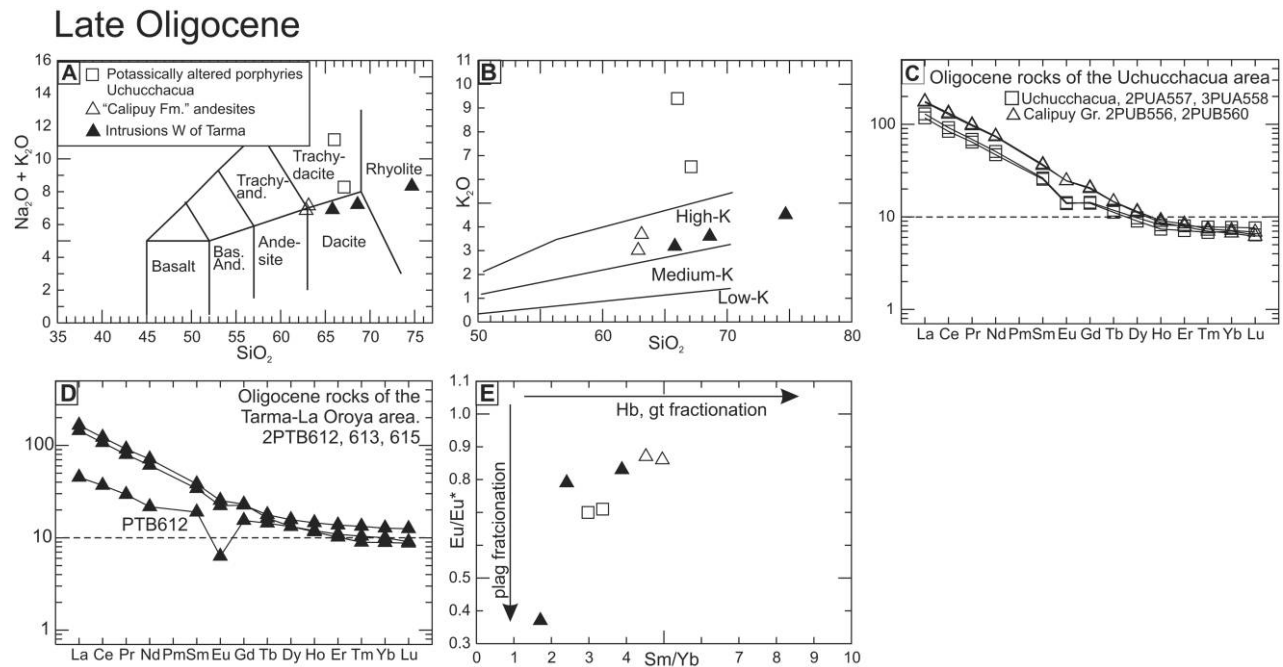


**Figure 5.** General geochemical characteristics of late Oligocene volcanic and intrusive rocks (see fig. 3 for references and abbreviations). *A*, Samples range from dacitic to rhyolitic compositions. The two Uchucchacua samples in the trachydacite field have experienced potassic alteration. *B*, Rocks are high-K calc-alkaline. Elevated K contents in the intrusive rocks from Uchucchacua are attributed to potassic alteration. *C*, *D*, Chondrite-normalized spider diagram for rare earth elements. *E*,  $\text{Eu}/\text{Eu}^*$  versus  $\text{Sm}/\text{Yb}$  diagram. No clear overall fractionation trend is evident.

1994). North of Domo de Yauli, early Miocene magmatism has not been confirmed, but at the Pallca prospect 40 km to the south of Huanzalá, a coarse-grained granodiorite porphyry with only a poor Ar isotope correlation age of  $18.7 \pm 2.5$  Ma (T. Bissig and T. D. Ullrich, unpub. data), may be the exception.

All rocks are high-K calc-alkaline in composition, albeit with the granodiorite from Vitis straddling the border to the trachydacite field (fig. 6A, 6B). Moreover, with the exception of the Vitis tonalitic sample, all rocks have more than 68 wt%  $\text{SiO}_2$  (fig. 6A, 6B). HREEs are generally not fractionated, with  $\text{Sm}/\text{Yb}$  between 2 and 2.7 and variable  $\text{Eu}/\text{Eu}^*$  ranging from 0.9 to 0.49. This is a reflection of the relatively felsic compositions of the rocks that have undergone feldspar fractionation (fig. 6C, 6D, 6F). However, two samples differ from the rest: the coarse porphyritic granodiorite from Pallca that has moderately fractionated HREEs and  $\text{Sm}/\text{Yb} = 3.7$  but only a shallow  $\text{Eu}/\text{Eu}^*$  of 0.82 and the peraluminous Canchayllo sample, with a  $\text{Sm}/\text{Yb}$  ratio of 3.73, a  $\text{Eu}/\text{Eu}^*$  ratio of 0.58 (fig. 6E, 6F), and low Sr concentrations of 165 ppm. The peraluminous character of this rock indicates sig-

nificant crustal contributions. The trace element signature is in permissive agreement with a significant melt contribution from a pelitic residue where garnet coexisted with plagioclase.

**Middle to Early Late Miocene Magmatism and Mineralization.** In the middle Miocene, widespread magmatism resumed and is represented by numerous small stocks and volcanic domes north and south of Domo de Yauli and the large Cordillera Occidental igneous complex around Cerro Tunshu (Cerro Tunshu igneous complex; Bissig et al. 2008; fig. 2). The 15–10-Ma middle to early late Miocene is metallogenetically the most significant period, with emplacement of numerous economic and subeconomic ore deposits related to shallow stocks (Bissig et al. 2008). However, economic mineralization occurred exclusively from Domo de Yauli to the north and includes (from south to north) the Morococha porphyry Cu mineralization at Ticlio (fig. 2, 16), the abandoned skarn deposit of Chungar (fig. 2, 12), the Colquijirca base metal lode and epithermal deposit (fig. 2, 9), the Iskaycruz skarn deposit (fig. 2, 6), the giant Cerro de Pasco Pb, Zn, and Cu carbonate replacement deposit (fig. 2, 10), and the giant Antamina Cu-Zn skarn deposit (fig.

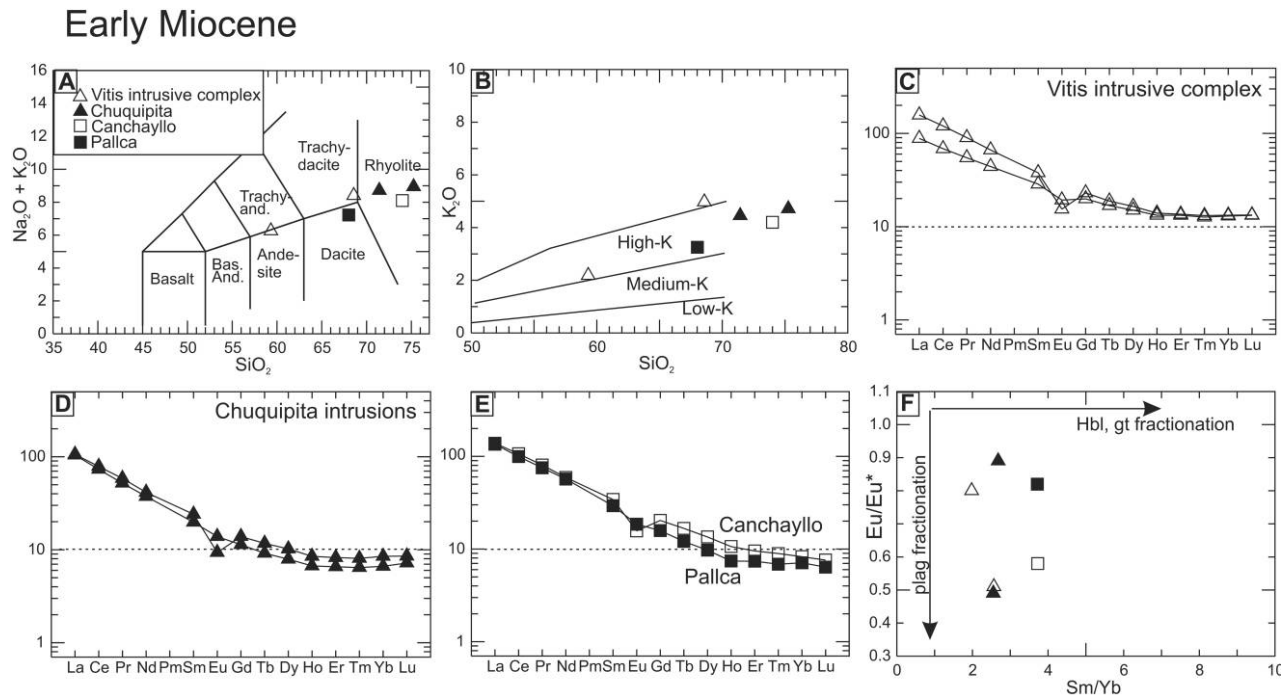


**Figure 6.** General geochemical characteristics of early Miocene intrusive rocks (see fig. 3 for references and abbreviations). *A*, With the exception of the Tonalite at Vitis, all samples range from dacitic to rhyolitic compositions. *B*, Rocks are high-K calc-alkaline, with the granodiorite of Vitis straddling the border to syenite. *C–E*, Chondrite-normalized spider diagrams for rare earth elements. *F*,  $\text{Eu}/\text{Eu}^*$  versus  $\text{Sm}/\text{Yb}$ . No clear overall fractionation trend is evident.

2, 2). Additional deposits of uncertain age may also have been emplaced in the same period and include the Yauliyacu and Casapalca Pb-Zn-Ag vein deposits (fig. 2, 18), as well as the abandoned Santander and Río Pallanga polymetallic deposits (fig. 2, 13, 15, respectively). Minor subeconomic Cu skarn mineralization at Mina Rey Salomón (fig. 2, 20) occurs at the periphery of a granodioritic intrusion of the Cerro Tunshu igneous complex.

The igneous rocks are high-K calc-alkaline rocks ranging from basaltic to rhyolitic compositions, with intermediate compositions being the most abundant (fig. 7). The most primitive rocks are diorites from the Marcapomacocha intrusion, 25 km northwest of La Oroya, a monzodiorite from the Cerro Tunshu intrusive complex, as well as a basalt from Río de la Virgen, approximately 10 km southwest of Chongos Alto. Andesitic rocks form the bulk of the intrusive rocks at Cerro Tunshu and Laguna Viccocha south of Domo de Yauli, whereas dacitic stocks are dominant in spatial and/or genetic association with the ore deposits north of Domo de Yauli (fig. 6A). High potassium contents in the Antamina rocks can readily be attributed to potassic alteration, on the basis of petrographic ob-

servation, whereas rocks of basaltic compositions are unaltered and in general have high primary alkali contents (fig. 7A). Rocks with >70%  $\text{SiO}_2$  appear to be related to skarn at Chungar and north of Uchucchacua.

HREE patterns of the middle to early late Miocene range from flat to steep (fig. 7C–7J). South of Domo de Yauli, the rocks from the Cerro Tunshu igneous complex generally have low  $\text{Sm}/\text{Yb}$  ratios from 1.6 to 2.6 and  $\text{Eu}/\text{Eu}^* = 0.73$  to 0.94 (avg. 0.84). However, the  $\text{SiO}_2$ -richest sample (69.5 wt%) from this complex, a garnet-bearing dacite dike, has a slightly positive Eu anomaly ( $\text{Eu}/\text{Eu}^* = 1.1$ ), fractionated HREE ( $\text{Sm}/\text{Yb} = 5.5$ ), and a low Sr content (242 ppm), which, together with the presence of phenocrystic garnet, suggest assimilation of meta-sedimentary material in which garnet and plagioclase coexisted in the residue.

In contrast to the large igneous complexes, the Río de la Virgen dacite domes and basaltic dike have distinctly higher  $\text{Sm}/\text{Yb}$  ratios (basalt: 3.72; dacite: 8.4), higher Sr contents (704 and 706 ppm, respectively), and only a very small Eu anomaly ( $\text{Eu}/\text{Eu}^* = 0.88$ –0.94). These rocks exhibit neither petrographic nor chemical evidence for peralumi-

## Middle to early late Miocene

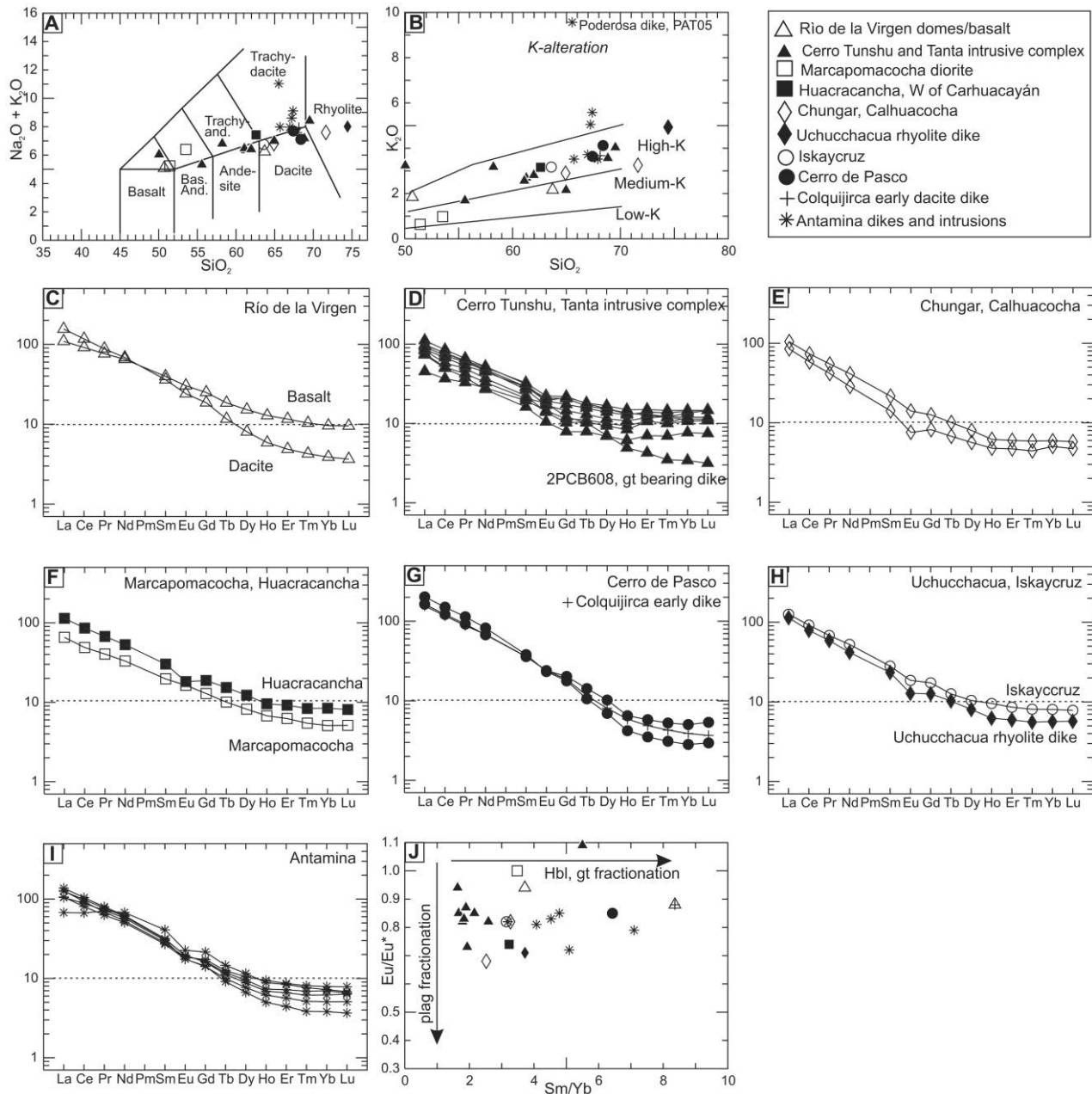


**Figure 7.** General geochemical characteristics of middle to early late Miocene intrusive rocks. A, Basaltic rocks are unaltered and rich in alkalines, whereas the rocks from Antamina with apparent trachydacite compositions have suffered potassic alteration. B, Rocks are high-K calc-alkaline, with the exception of one monzodioritic rock from the Cerro Tunshu intrusive complex. High potassium contents of the rocks from Antamina can be explained by potassic alteration. C-I, Chondrite-normalized spider diagrams for rare earth elements. J, Eu/Eu\* versus Sm/Yb diagram. The rocks overall follow a garnet/hornblende fractionation trend.

nous character. The REE pattern (fig. 7C) is therefore interpreted as evidence for a plagioclase-free but garnet-bearing residue of the primitive source rock in the lower crust.

North of Domo de Yauli, rocks of basaltic composition with relatively high Sm/Yb ratios occur at Marcapomacocha (Sm/Yb = 3.48; Sr = 679 ppm; Eu/Eu\* = 1), again an indication of garnet stability

in the lower crustal source rocks. Felsic rocks associated with modest-size polymetallic ore deposits at Chungar and Iskaycruz exhibit only minor to moderate middle REE (MREE)/HREE fractionation but low overall MREE and HREE abundances ( $\text{Sm}/\text{Yb} = 2.5\text{--}3.2$ ; fig. 7E, 7J), in marked contrast to rocks associated with the giant deposits of Colquijirca, Cerro de Pasco, and Antamina that have consistently high  $\text{Sm}/\text{Yb}$  ratios (Colquijirca: 8.3; Cerro de Pasco: 6.4–12.1; Antamina: 4–7.1) and minor Eu depletions ( $\text{Eu}/\text{Eu}^* = 0.8\text{--}0.85$ ). The rhyolite dike north of Uchucchacua exhibits a high  $\text{Sm}/\text{Yb}$  ratio of 3.7 combined with a  $\text{Eu}/\text{Eu}^*$  value of 0.71, with the latter possibly indicating moderate feldspar fractionation at shallow crustal levels.

**Late Miocene Magmatism and Mineralization.** Late Miocene magmatism is represented by dikes, domes, small stocks, and, at Yauricocha, intrusions of considerable size. These igneous rocks are scattered over the entire study area and include domes near Chongos Alto (40 km east of Cordillera Occidental) as well as dikes and intrusions along the axis of the continental divide. Most rocks are of dacitic to rhyolitic composition, straddling the border between trachydacite and dacite in the total alkali versus silica diagram (fig. 8A). One sample from the Anamaray intrusion and a dome of the Herú Formation are slightly more primitive and plot as trachyandesite, albeit close to the andesite field. Significant polymetallic mineralization occurred in the late Miocene in the vein deposits of Domo de Yauli (San Cristóbal; fig. 2, 17), probably at Uchucchacua (fig. 2, 5) and at the carbonate replacement deposits of Yauricocha (fig. 2, 22), as well as in the nearby mineralized Purisima Concepción area (Alvarez and Noble 1988). Epithermal mineralization is known from the abandoned Carhuacayán mine (fig. 2, 14), skarn mineralization from Raura ( $8.2 \pm 0.2$  Ma; Noble and McKee 1999; fig. 2, 4), and Huanzalá (fig. 2, 3).

Trace element patterns (fig. 8C–8I) of the late Miocene rocks exhibit little variation. HREEs are generally fractionated, with  $\text{Sm}/\text{Yb}$  ratios between 3.7 and 7.5. However, Soler (1991) reported  $\text{Sm}/\text{Yb}$  ratios of up to 10.1 for the 5.1-Ma ignimbrite of Bosque de Piedra south of Cerro de Pasco (fig. 8H, 8I). In contrast, Sr concentrations are generally high (600–1055 ppm) and Eu anomalies are relatively minor (0.79–0.9) for all late Miocene rocks, which indicates that residual hornblende and garnet, rather than plagioclase, controlled the trace element patterns of the melt.

## Radiogenic Isotope Signatures

**Igneous Rocks.** We analyzed nine Cenozoic igneous rocks for radiogenic Sr and Pb isotopes (figs. 9, 10) to complement published data from Domo de Yauli (Chiaradia and Fontboté 2002; Beuchat 2003), Atacocha (Gunnesch et al. 1990; Soler and Rotach-Toulhoat 1990), Chungar, Calhuacocha, Bosque de Piedra, and Yanamate southeast of Cerro de Pasco (Soler and Rotach-Toulhoat 1990). Given the relatively young age of our samples coupled with the low Rb-Sr ratios inherent to plagioclase, the Pb and Sr isotope ratios have not been corrected to initial values and are considered to be close to the original composition. Soler and Rotach-Toulhoat (1990) presented only age-corrected Sr isotopic data for similarly aged whole-rock samples. In addition, Pb isotopic compositions for Mesozoic sedimentary rocks (Gunnesch et al. 1990), broad-scale Pb isotopic fields for the Cretaceous and Tertiary Coastal Batholith of Peru (Mukasa 1986), and Paleozoic and Precambrian rocks from the Eastern Cordillera of Peru (Macfarlane 1999; Macfarlane et al. 1999; Haeberlin 2002) are available.

The  $^{87}\text{Sr}/^{86}\text{Sr}$  ratios range from 0.7038 for the late Eocene diorite intrusion at Chaucha to 0.7089 for the middle Miocene garnet-bearing dacite dike near Cerro Tunshu (fig. 9). An overall increase of  $^{87}\text{Sr}/^{86}\text{Sr}$  with younger age is evident, although the initial Sr ratios of similarly aged samples vary widely. We observed no correlation of elevated Sr isotopic influence with silica content. The most mafic rock analyzed from the Cerro Tunshu intrusive complex (diorite, sample 2PCB607) has a relatively high  $^{87}\text{Sr}/^{86}\text{Sr}$  ratio of 0.7064. This contrasts with that of the other mafic rocks, including the middle Miocene basalt from Río de la Virgen ( $^{87}\text{Sr}/^{86}\text{Sr} = 0.7048$ ; sample 2PYB524), the late Eocene Chaucha diorite ( $^{87}\text{Sr}/^{86}\text{Sr} = 0.7038$ ; sample PYB540), and Señal Raco west of Cerro de Pasco ( $^{87}\text{Sr}/^{86}\text{Sr} = 0.70425$ ; Soler and Rotach-Toulhoat 1990). The Eocene Huacravilca granodiorite intrusion, the late Miocene Exito granodiorite stock at Yauricocha, a dacite dome of the Herú Formation, a dacite dome at Carhuacayán, and the Taco Porphyry at Antamina all have intermediate  $^{87}\text{Sr}/^{86}\text{Sr}$  ratios between 0.7052 and 0.7057, within the same range as the ratios from Chungar, Calhuacocha, and Yanamate (fig. 9; Soler and Rotach-Toulhoat 1990). The more radiogenic Sr ratios occur in the late Miocene Domo de Yauli intrusions (0.7056–0.7065; Beuchat 2003), Atacocha (0.7065; Soler and Rotach-Toulhoat 1990), and the Cerro Tunshu intrusive

## Late Miocene

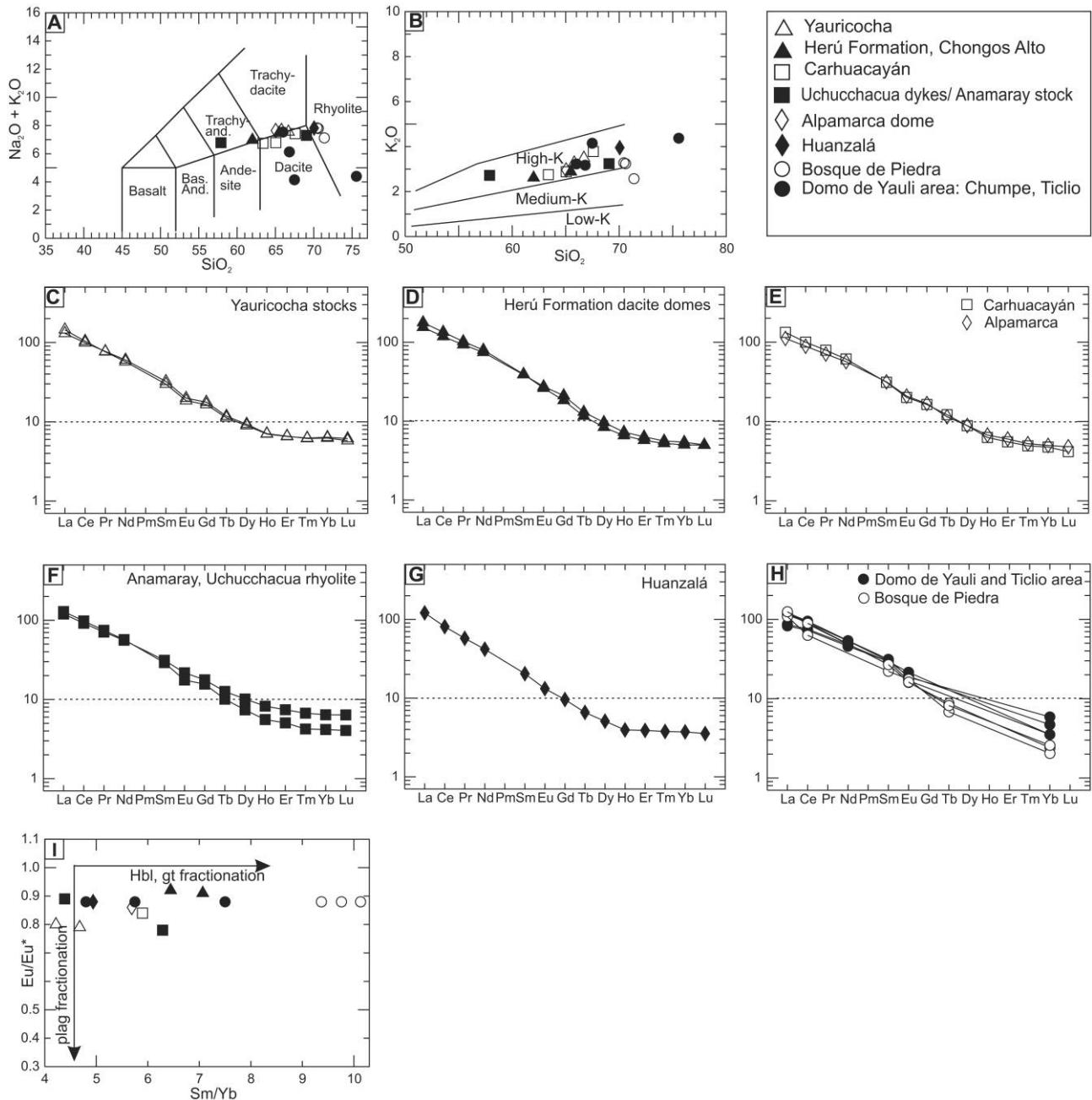


**Figure 8.** General geochemical characteristics of late Miocene intrusive and volcanic rocks. The analytical data for the samples from the Domo de Yauli and Ticlio areas are from Beuchat (2003), and those for Bosque de Piedra are from Soler (1991; see fig. 3 for references and abbreviations). A, Low alkali concentrations can be attributed to argillic and advanced argillic alteration at San Cristóbal and Morococha (Ticlio area). B, Rocks are high-K calc-alkaline. C–H, Chondrite-normalized spider diagrams for rare earth elements. I,  $\text{Eu}/\text{Eu}^*$  versus  $\text{Sm}/\text{Yb}$ . The rocks overall follow a garnet/hornblende fractionation trend.

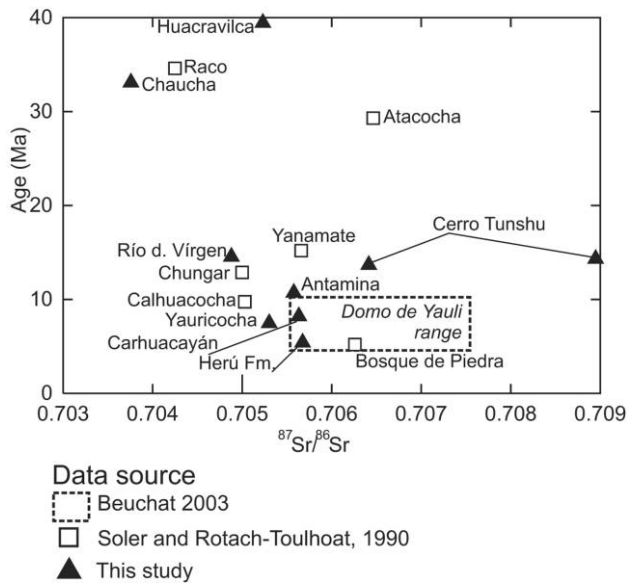


**Figure 9.** Evolution of the Sr isotopic composition from the Eocene to the late Miocene. Data sources as indicated.

complex (0.7064–0.7089), ca. 20 km southwest of Domo de Yauli.

Lead isotopes in general correlate with the Sr isotopes. The lowest  $^{207}\text{Pb}/^{204}\text{Pb}$  igneous rocks are the Río de la Virgen basalt and the Chaucha diorite intrusion, which in the  $^{207}\text{Pb}/^{204}\text{Pb}$  versus  $^{206}\text{Pb}/^{204}\text{Pb}$  isotope diagram (fig. 10B) are the only samples that fall below the average crustal growth curve of Stacey and Kramers (1975). Albeit younger, these rocks were largely derived from a source similar to that of the Cretaceous and early Tertiary coastal batholith (Mukasa and Tilton 1985), to the immediate west of the study area. This source is generally assumed to be an enriched mantle or melting assimilation storage homogenization environment at the base of the crust (Macfarlane 1999; Chiaradia and Fontboté 2002). In contrast, the other samples and published analyses (Chiaradia and Fontboté 2002) plot above the average crustal growth curve and overlap the fields for sedimentary rocks reported herein, as well as for Carboniferous granitoids and pre-Carboniferous metamorphic rocks (fig. 10) that formed part of the Paleozoic Gondwanan margin.

In contrast to the Sr isotope systematics, the Pb isotopes indicate that the Río de la Virgen basalt has somewhat lower  $^{206}\text{Pb}/^{204}\text{Pb}$  than the Chaucha diorite. Two Cerro Tunshu intrusive complex samples are at the high  $^{206}\text{Pb}/^{204}\text{Pb}$  end of the Pb iso-

topic spectrum, with the highest  $^{206}\text{Pb}/^{204}\text{Pb}$  from the garnet-bearing dacite dike; these values are consistent with the elevated Sr isotopic compositions. The Atacocha quartz diorite from 130 km north of Cerro Tunshu (Gunnesch et al. 1990) occupies a similar position in  $^{207}\text{Pb}/^{204}\text{Pb}$  versus  $^{206}\text{Pb}/^{204}\text{Pb}$  space, whereas the Domo de Yauli Miocene intrusions have an intermediate range, albeit with somewhat higher  $^{207}\text{Pb}/^{204}\text{Pb}$ . Compared with those for Cenozoic igneous rocks, the lead compositions for Paleozoic and Mesozoic sedimentary rocks from the Domo de Yauli and Milpo Atacocha area occupy a much wider Pb isotopic compositional range (Gunnesch et al. 1990) that extends to significantly higher  $^{206}\text{Pb}/^{204}\text{Pb}$  ratios than the Cenozoic igneous rocks, and these rocks are more similar to the Paleozoic and older rocks in the Eastern Cordillera (fig. 10), from which some of their detritus must have been derived (Benavides 1999).

The overall Sr and Pb isotopic compositions of the igneous rocks indicate a generally moderate crustal assimilation of ancient radiogenic rocks, potentially similar to upper crustal sources such as the sedimentary rock units hosting the Cenozoic intrusions or the Paleozoic and older crystalline basement. There is no systematic increase of such assimilation toward the east or at specific time intervals, as igneous rocks with widely varying isotopic signatures have been emplaced in different locations.

**Ore Lead.** Lead isotopic compositions of sulfide minerals from magmatic-related ore deposits have widely been used as a proxy for Pb isotopic compositions of associated igneous rocks (Macfarlane 1999; Tosdal et al. 1999). Ore lead isotopic data from 14 different polymetallic deposits or prospects are available (Gunnesch et al. 1990; Fontboté and Bendezú 2001; Chiaradia and Fontboté 2002; Beuchat 2003; Baumgartner 2007; this study). The data, overall, lie on an array between the range of Pb isotopic compositions of the igneous rocks and a higher  $^{208}\text{Pb}/^{204}\text{Pb}$  and  $^{207}\text{Pb}/^{204}\text{Pb}$  source (fig. 11). The latter best matches the compositions for Paleozoic and Mesozoic siliciclastic sedimentary rocks or the Carboniferous and older crystalline basement (fig. 11; Gunnesch et al. 1990; Macfarlane 1999; Macfarlane et al. 1999) from which the siliciclastic rocks were derived. The mixing trend is well recognized throughout the central Andes in Tertiary ore deposits and defines the Province II Pb isotopic compositions (Macfarlane et al. 1990; Macfarlane 1999; Tosdal et al. 1999; Tosdal and Munizaga 2003). It is most clearly shown by the Atacocha-Milpo districts, as well as by the Cerca-puquio deposit (see also Macfarlane 1999). The

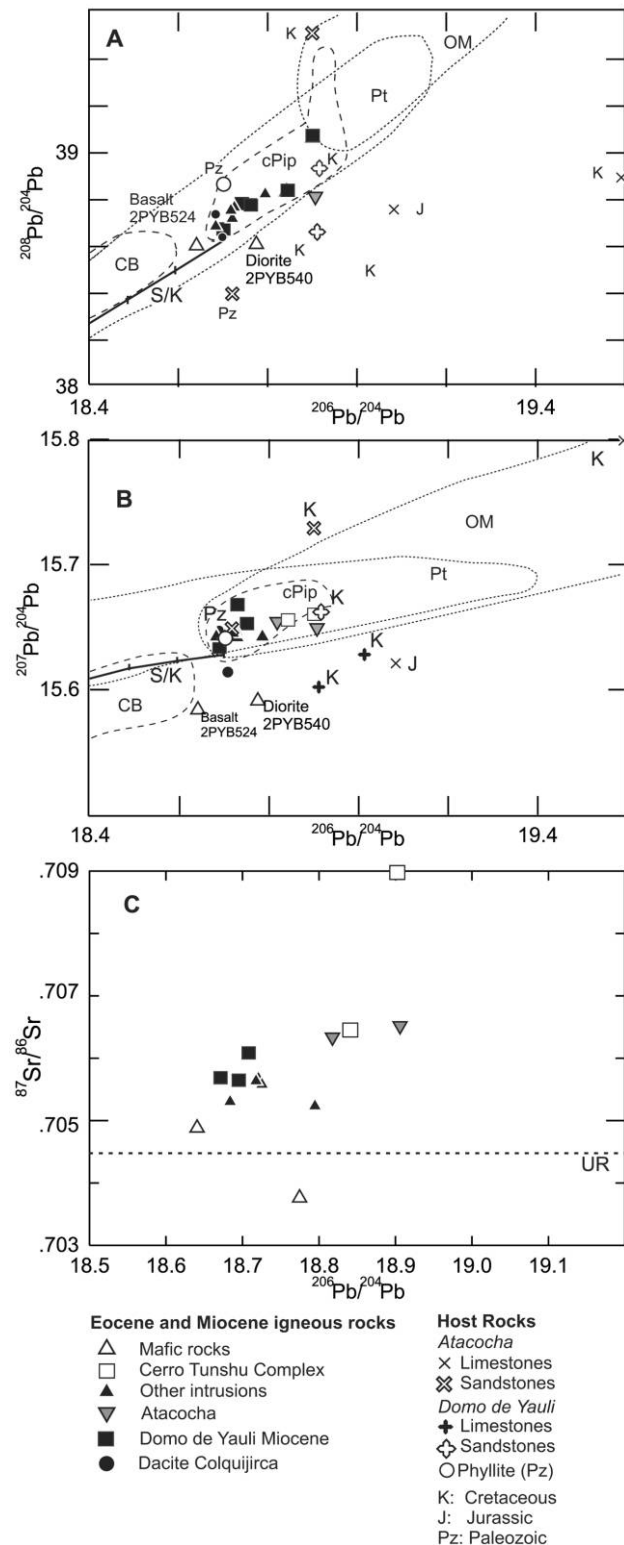


**Figure 10.** Pb and Sr isotopic data for igneous rocks from central Peru. Data sources are as follows: all host rocks and Atacocha intrusion: Gunnesch et al. (1990); Domo

de Yauli Miocene intrusions: Beuchat (2003); all others: this study. *A*, Uranogenic Pb isotope diagram. *S/K* = Crustal evolution curve from Stacey and Kramers (1975). *B*, Thorogenic Pb isotope diagram. *C*,  $^{87}\text{Sr}/^{86}\text{Sr}$  versus  $^{206}\text{Pb}/^{204}\text{Pb}$  isotopes. *UR* = uniform reservoir.

Atacocha-Milpo array is parallel to the Cercapuquio array but shifted to higher  $^{206}\text{Pb}/^{204}\text{Pb}$  ratios, which is consistent with the Pb isotopic compositions of the intrusions at Atacocha (Gunnesch et al. 1990) compared with the Pb isotopic composition of the Huacravilca intrusion at 4 km from Cercapuquio (sample 2PYB518). The deposits can be loosely grouped into two populations with respect to their Pb isotopic compositions. Group 1 includes Milpo, Atacocha, Uchucchacua, Iskaycruz, Cercapuquio, Casapalca, and Pallca and is characterized by a range of Pb isotopic compositions varying from  $^{206}\text{Pb}/^{204}\text{Pb} = 18.680$  to  $18.940$ , from  $^{207}\text{Pb}/^{204}\text{Pb} = 15.612$  to  $15.724$ , and from  $^{208}\text{Pb}/^{204}\text{Pb} = 38.667$  to  $39.219$  (fig. 11). These ore lead isotopic ratios extend from values similar to those of Neogene igneous rocks to those of more radiogenic upper crustal Paleozoic rocks. Group 2 includes Antamina, Huanzalá, Contonga, Colquijirca, and Yauricocha and is characterized by overall lead compositions close to those of the compositional field for Neogene igneous rocks, not exceeding  $^{206}\text{Pb}/^{204}\text{Pb}$  values of  $18.753$ ,  $^{207}\text{Pb}/^{204}\text{Pb}$  values of  $15.675$ , and  $^{208}\text{Pb}/^{204}\text{Pb}$  values of  $38.854$ . The Morococha, San Cristóbal, and Cerro de Pasco deposits may be transitional between groups 1 and 2 on the basis of their Pb isotope signature. Within group 2, where data exist (Yauricocha, Antamina), ore lead isotopic values are similar to the Pb isotope values of plagioclase in the cogenetic igneous rocks. However, caution must be exercised with the interpretation of the group 2 data, as it is unclear whether the differences in group 1 represent contrasting Pb source(s) or whether they are an artifact of the limited sampling of group 2 deposits.

## Discussion

**The Geochemical Evolution with Time.** Sm/Yb values show an overall increase with younger age (fig. 12). A clear trend from low ratios in the Eocene to values ranging from 3 to 10 in the late Miocene is apparent. A similar trend is seen with Sr/Y ratios, where the values for Eocene rocks are mostly below

de Yauli Miocene intrusions: Beuchat (2003); all others: this study. *A*, Uranogenic Pb isotope diagram. *S/K* = Crustal evolution curve from Stacey and Kramers (1975). *B*, Thorogenic Pb isotope diagram. *C*,  $^{87}\text{Sr}/^{86}\text{Sr}$  versus  $^{206}\text{Pb}/^{204}\text{Pb}$  isotopes. *UR* = uniform reservoir.

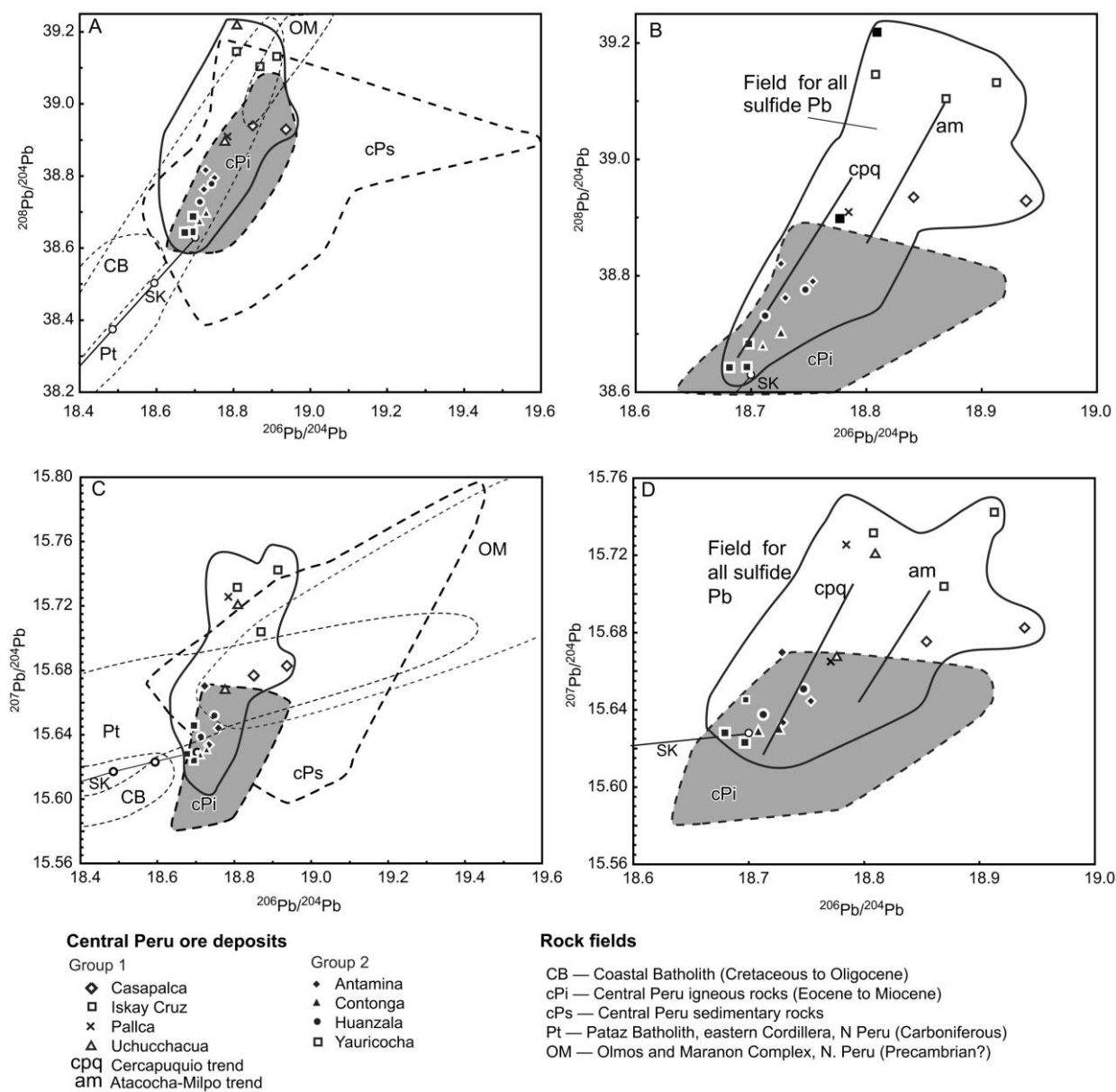


**Figure 11.** Pb isotopic compositions for ore minerals from central Peru relative to igneous rocks and basement units (see fig. 10 for more detail). Note: all data define a sulfide compositional field, but only data from this study are plotted as individual points. Data sources are as follows: Casapalca, Cercapuquio, Atacocha: Gunnesch et al. (1990); San Cristobal: Gunnesch et al. (1990), Beuchat (2003); Morococha: Gunnesch et al. (1990), this study; Milpo: mostly Gunnesch et al. (1990), two data points from this study; remaining samples: this study. *A*, Uranogenic diagram showing ore lead compositions relative to different reference fields. *S/K* = crustal evolution curve from Stacey and Kramers (1975). *B*, Enlargement of *A*, showing compositional trends in the sulfide lead data. *C*, *D*, Thorogenic diagram, equivalent to *A* and *B*.

40 but range from 40 to 110 in the late Miocene. Rather than a general increase of Sm/Yb and Sr/Y ratios, a wider spreading of values with younger age can be observed (fig. 12). Middle Miocene rocks range from Sm/Yb = 1.5 to 9 and from Sr/Y = 10

to 130, whereas low Sm/Yb ratios are absent only in the late Miocene (fig. 12). The pattern of Sr/Y ratios is similar. The unusually low values for the Chumpe intrusion (San Cristobal; Beuchat 2003) are readily explained by hydrothermal alteration of

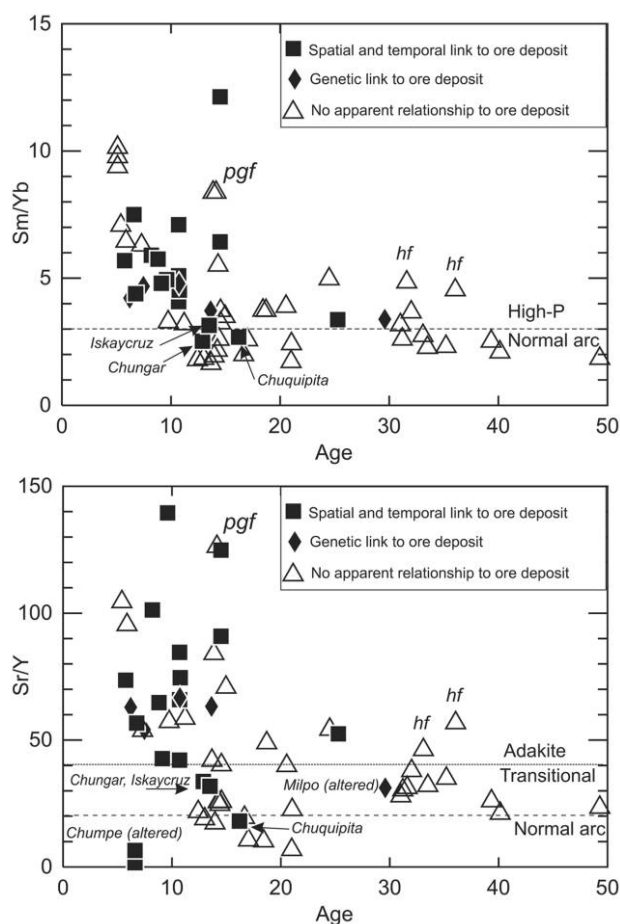


**Figure 12.** Trace element compositional evolution with time. *A*, Sm/Yb ratios, representing heavy rare earth element fractionation, versus age. "High-P" versus "normal arc" boundary is drawn on the basis of empiric relationships in the Chilean flat slab segment (Kay et al. 1999; Bissig et al. 2003). Igneous rocks spatially and temporally related to mineralization at Chuquipita, Chungar, and Iskaycruz fall into the normal arc field, whereas all other deposits are associated with magmas that have been generated under high pressures. *hf* = samples exhibiting evidence for hornblende fractionation; *pgf* = samples exhibiting evidence for assimilation of pelitic material. *B*, Sr/Y ratios versus age. Boundaries separating normal arc, transitional, and adakite fields are from Defant and Drummond (1993). Note that Chungar, Iskaycruz, and Chuquipita fall in the transitional field. The low Sr/Y ratios for Milpo and Chumpe (Domo de Yauli; Beuchat 2003) are due to hydrothermal alteration.

the analyzed sample (fig. 12). The general trend toward greater spreading of Sm/Yb and Sr/Y ratios with younger age is also apparent after disregarding samples where significant assimilation of midcrustal material (possibly pelite derived) or important

fractional crystallization of hornblende may have occurred.

Middle Miocene intrusions near the Cordillera Occidental have generally lower Sm/Yb ratios compared with those of domes and intrusions farther east. South of Domo de Yauli, generally low La/Yb, Sm/Yb, and Sr/Y trace element ratios occur in the Cerro Tunshu igneous complex and nearby intrusions, whereas middle Miocene dacite domes and Río de la Virgen basalt exhibit higher values. North of Domo de Yauli intrusions, high Sm/Yb and Sr/Y ratios are the rule except for Chungar, with Sr/Y = 33.6 and Sm/Yb = 2.52. The low MREE and HREE abundances at Chungar indicate that hornblende ± garnet probably was present in the source. If we assume that garnet in the residuum played a major role in the rocks with Sr/Y > 40 and Sm/Yb > 3, the trace element signature may be used as a proxy for crustal thickness (e.g., Hildreth and Moorbath 1988; Kay et al. 1991). One may speculate that the crust beneath the Cordillera Occidental was, in the middle Miocene, thinner than 45 km, in contrast to areas 20–50 km east of the continental divide at the same time. However, the Sr and Pb isotope signatures of the Cerro Tunshu intrusive complex rocks and some Domo de Yauli intrusions indicate that these rocks have experienced more crustal assimilation or have interacted with more ancient crustal rocks than the igneous rocks elsewhere in the Cordillera Occidental. This may be attributed to a more compressive tectonic regime that may have favored crustal assimilation in this area or the local age and composition of the crust. Thus, REE and trace element ratios of Eocene and Neogene igneous rocks in central Peru are not controlled by crustal thickness alone but in some cases also by melting, assimilation, and fractionation processes during the ascent of the magmas through a heterogeneous crust.

**Metallogenic Relationships.** The majority of rocks spatially and temporally related with the known ore deposits of the central Peruvian cordillera exhibit a relatively low Y content but elevated Sr/Y, Sm/Yb, and  $La_n/Yb_n$  ratios (fig. 13A–13F), whereas rocks apparently unrelated to mineralization exhibit a wide compositional range with respect to these trace element ratios. Figure 13G shows Th versus Y, both normalized to  $TiO_2$ . Th is enriched and Y depleted in apparently fertile igneous rocks. Th is extremely incompatible in a garnet-bearing high-pressure residue (Blundy and Wood 2003), whereas Y would be compatible in such an environment. Y and Th combined hence indicate that potentially fertile magmas were generated under high pressures. With exception of

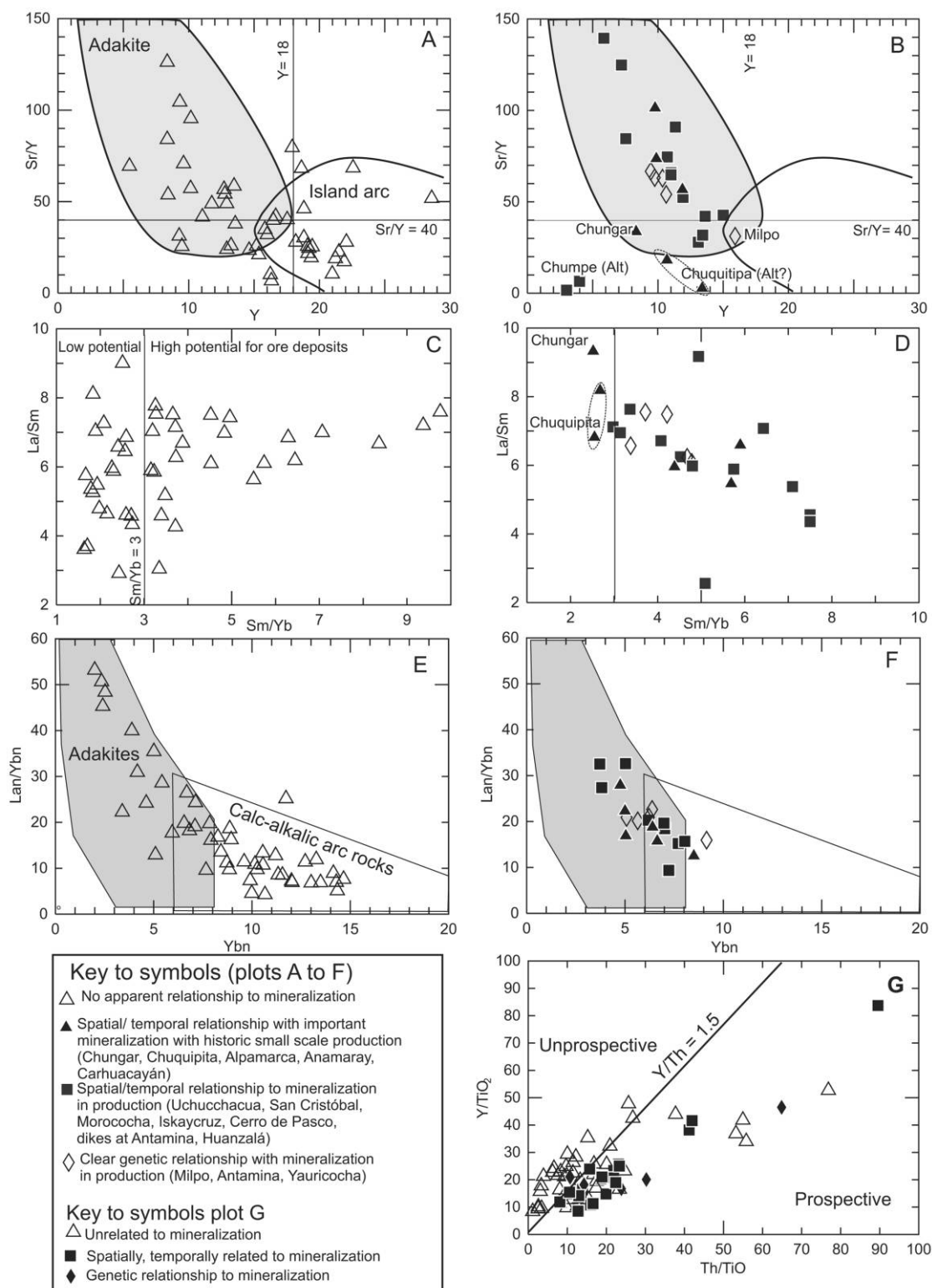


**Figure 13.** Discrimination diagrams for identifying igneous rocks where garnet and/or hornblende fractionation occurred. Igneous rocks spatially, temporally, and genetically related to ore deposits (*right*) generally fall into the fields for adakites as defined by Defant and Drummond (1993) and Martin (1999). *G*, Further discrimination diagram on the basis of Y versus Th, normalized by TiO<sub>2</sub>. Boundary between prospective and unprospective fields is based empirically on the data set presented herein.

Milpo, all igneous rocks associated with mineralization exhibit  $Y/Th \leq 1.5$ .

The general association of mineralization with melts generated under high pressures has been widely recognized around the Pacific (e.g., Thieblemont et al. 1997; Sajona and Maury 1998; Kay and Mpodozis 2001; Bissig et al. 2003). There are, however, igneous rocks associated with ore deposits that do not conform well to a high-P residue: most notably at Milpo, Chungar, and Iskaycruz. The mineralization at Milpo occurred in the early Oligocene when the crust may have been thinner than in the Miocene and melts evolved from a garnet-free residuum, whereas Chungar and Iskaycruz were emplaced in the middle and early late Miocene in the Cordillera Occidental when the continental crust in central Peru probably was  $>45$  km thick. The apparent contradiction between the observed trace element patterns and inferred crustal thickness is attributed to extensive middle and upper crustal interaction of the ascending magmas. In this context, Pb isotopes on ores from throughout the study area may represent a useful tool to understand the trace element chemistry of igneous rocks associated with the deposits. The ore deposits associated with igneous rocks with relatively low Sm/Yb ratios from 2.97 to 4.3 for deposits where Pb isotopic constraints are available (i.e., Milpo, Iskaycruz, Uchucchacua) exhibit  $^{206}Pb/^{204}Pb$ ,  $^{207}Pb/^{204}Pb$ , and  $^{208}Pb/^{204}Pb$  ratios ranging from compositions typical for Eocene to Miocene igneous rocks to relatively radiogenic values indicative of a potential derivation of some lead from the Mesozoic and older upper crustal sedimentary, igneous, and metamorphic rocks. The deposits (i.e., Antamina, Colquijirca, Yauricocha) associated with lower  $^{207}Pb/^{204}Pb$  and  $^{208}Pb/^{204}Pb$  ratios similar to the Pb isotopic composition of Cenozoic igneous rocks are related to igneous rocks with generally higher Sm/Yb ratios, ranging from 4.2 to 8.3. This general association of trace element chemistry with lead isotopes, although possibly an artifact of the limited database, may indicate an important control of the degree of crustal assimilation on the fertility of igneous systems. It is apparent that large deposits such as Antamina, Colquijirca, and Yauricocha are related to magmas with limited interaction with the middle and upper crust and were largely mineralized by fluids of magmatic origin. Other generally smaller deposits including Milpo, Uchucchacua, and Iskaycruz are associated with magmas that have interacted to a more significant degree with the crust.

### Concluding Remarks

Central Peruvian polymetallic ore deposits are associated with high-K calc-alkaline igneous rocks that have undergone variable degrees of crustal assimilation during their ascent through a heterogeneous continental crust. Despite the heterogeneity, if the igneous rocks are evaluated on a mineral district scale and care is taken to understand the geologic relationships as well as the petrogenesis, whole-rock geochemistry can be a valuable tool for mineral exploration. On the basis of the data presented herein and geochronological constraints from Bissig et al. (2008), the following relationships are proposed: magmatic rocks potentially associated with a large polymetallic ore deposit in central Peru are (1) middle and late Miocene in age or located in the Uchucchacua-Milpo transect and (2) dacitic in composition with high ( $>4$ ) Sm/Yb and low ( $\leq 1.5$ ) Y/Th ratios and only limited crustal contamination. Pb isotopes of ore minerals indicate a largely magmatic fluid source for the large Miocene deposits of Antamina, Cerro de Pasco, and Colquijirca. Some generally smaller ore deposits may also be associated with magmas with moderate Sm/Yb ratios (2.7–4), especially if they are located in the Uchucchacua-Milpo transect and are Oligocene or older in age. Magmas associated with these deposits may have undergone more significant crustal contamination. Rocks with high Sm/Yb ratios are not necessarily prospective and have to be evaluated critically for shallow-level hornblende fractionation or extensive assimilation of pelitic crustal material.

### ACKNOWLEDGMENTS

Financial and logistical support was provided by Anglo American, Exploration, Compañía de Minas Buenaventura, Compañía Minera Antamina, BHP Billiton, Falconbridge, Phelps Dodge, and Teck Cominco, as well as by the Natural Science and Engineering Research Council of Canada. T. Bissig would also like to thank the Swiss National Science Foundation for a stipend. D. Weis is thanked for radiogenic isotope analysis and comments on earlier versions of the manuscript, P. Pariguana for field assistance, and L. Jofré for the drafting of one figure. P. Hollings and one anonymous reviewer are acknowledged for their comments and suggestions, which helped to improve and shorten this article. This is Mineral Deposit Research Unit contribution 233.

## REFERENCES CITED

- Alvarez, A., and Noble, D. C. 1988. Sedimentary rock-hosted disseminated precious metal mineralization at Purísima Concepción, Yauricocha district, central Peru. *Econ. Geol.* 83:1368–1378.
- Baumgartner, R. 2007. Sources and evolution in space and time of hydrothermal fluids at the Cerro de Pasco cordilleran base metal deposit, central Peru. PhD thesis, University of Geneva. *Terre Environ.* 66, 167 p.
- Baumgartner, R.; Fontboté, L.; and Vennemann, T. 2008. Mineral zoning and geochemistry of epithermal polymetallic Zn-Pb-Ag-Cu-Bi mineralization at Cerro de Pasco, Peru. *Econ. Geol.* 103:493–537.
- Benavides, V. 1999. Orogenic evolution of the Peruvian Andes: the Andean cycle. In Skinner, B. J., ed. *Geology and ore deposits of the central Andes*. *Soc. Econ. Geol. Spec. Publ.* 7:61–107.
- Bendezú, R.; Baumgartner, R.; Fontboté, L.; Page, L.; Pecsckay, Z.; and Spikings, R. 2004. The Cerro de Pasco-Colquijirca "super-district," Peru: ~2 m.y. of pulsed high-sulphidation hydrothermal activity. Society of Economic Geologists biannual meeting (Perth, Sept. 2004), *Proc.*, p. 340–342.
- Bendezú, R.; Page, L.; Spikings, R.; Pecsckay, Z.; and Fontboté, L. 2008. New  $^{40}\text{Ar}/^{39}\text{Ar}$  alunite ages from the Colquijirca district, Peru: evidence of a long period of magmatic  $\text{SO}_2$  degassing during formation of epithermal Au-Ag and cordilleran polymetallic ores. *Mineral. Deposit.* 43:777–789.
- Beuchat, S. 2003. Geochronological, structural, isotope and fluid inclusion constraints of the polymetallic Domo de Yauli district, Peru. *Terre Environ.* 41, 130 p.
- Beuchat, S.; Moritz, R.; and Pettke, T. 2004. Fluid evolution in the W-Cu-Zn-Pb San Cristobal vein, Peru: fluid inclusion and stable isotope evidence. *Chem. Geol.* 210:201–224.
- Bissig, T.; Clark, A. H.; Lee, J. K. W.; and Von Quadt, A. 2003. Petrogenetic and metallogenetic responses to Miocene slab flattening: new constraints from the El Indio-Pascua Au-Ag-Cu belt, Chile/Argentina. *Mineral. Deposit.* 38:844–862.
- Bissig, T.; Ullrich, T. D.; Tosdal, R. M.; Friedman, R.; and Ebert, S. 2008. The time-space distribution of Eocene to Miocene magmatism in the central Peruvian polymetallic province and its metallogenetic implications. *J. S. Am. Earth Sci.* 26:16–35.
- Blundy, J., and Wood, B. 2003. Mineral-melt partitioning of uranium, thorium and their daughters. *Rev. Mineral. Geochem.* 52:59–123.
- Bussell, M. A.; Alpers, C. N.; Petersen, U.; Shepherd, T. J.; Bermudez, C.; and Baxter, A. N. 1990. The Ag-Mn-Pb-Zn vein, replacement and skarn deposits of Uchucchacua, Peru: studies of structure, mineralogy, metal zoning, Sr isotopes and fluid inclusions. *Econ. Geol.* 85:1348–1383.
- Carrascal, R., and Sáez, J. 1990. Stratabound polymetallic ore deposits of the Santa metalotect in the Huanzalá and Pachapaqui mining areas in central Peru. In Fontboté, L.; Amstutz, G. C.; Cardozo, M.; Cedillo, E.; and Frutos, J., eds. *Stratabound ore deposits in the Andes*. Berlin, Springer, p. 556–568.
- Cedillo, E. 1990. Stratabound lead-zinc deposits in the Jurassic Chaucha Formation, central Peru. In Fontboté, L.; Amstutz, G. C.; Cardozo, M.; Cedillo, E.; and Frutos, J., eds. *Stratabound ore deposits in the Andes*. Berlin, Springer, p. 538–553.
- Cedillo, E., and Tejada, J. 1988. Yacimientos estratoligados de plomo y zinc en la formación Chaucha del Jurásico Superior: Cercapuquio, Junín. *Bol. Soc. Geol. Peru* 78:35–43.
- Chiaradia, M., and Fontboté, L. 2002. Lead isotope systematics of Late Cretaceous–Tertiary Andean arc magmas and associated ores between 10°N and 40°S: evidence for latitudinal mantle heterogeneity beneath the Andes. *Terra Nova* 14:337–342.
- Cobbing, E. J. 1973. *Geología de los cuadrángulos de Barranca, Ambar, Oyón, Huacho, Huaral y Canta*. Lima, Bol. Serv. Geol. Minas, 172 p.
- Defant, M. J., and Drummond, M. S. 1993. Mount St. Helens: potential example of the partial melting of the subducted lithosphere in a volcanic arc. *Geology* 21: 547–550.
- Farrar, E., and Noble, D. C. 1976. Timing of late Tertiary deformation in the Andes of Peru. *Geol. Soc. Am. Bull.* 87:1247–1250.
- Flores, G. 1990. Geology of Iscaycruz ore deposits in the Santa Formation, central Peru. In Fontboté, L.; Amstutz, G. C.; Cardozo, M.; Cedillo, E.; and Frutos, J., eds. *Stratabound ore deposits in the Andes*. Berlin, Springer, p. 584–594.
- Fontboté, L., and Bendezú, R. 2001. The carbonate-hosted San Gregorio and Colquijirca (Zn-Pb-Ag) deposits (central Peru) as products of an epithermal high sulfidation system. International Congress of Prospectors and Explorers (PROEXPLO), CD-ROM. Lima, Instituto de Ingenieros de Minas del Peru, p. 19.
- Gunnesch, K. A., and Baumann, A. 1984. The Atacocha district, central Peru: some metallogenetic aspects. In Wauschkuhn, A.; Kluth, C.; and Zimmermann, R. A., eds. *Syngeneses and epigenesis in the formation of mineral deposits*. Heidelberg, Springer, p. 448–456.
- Gunnesch, K. A.; Baumann, A.; and Gunnesch, M. 1990. Lead isotope variations across the central Peruvian Andes. *Econ. Geol.* 85:1384–1401.
- Gutscher, M.-A.; Olivet, J.-L.; Aslanian, D.; Eissen, J.-P.; and Maury, R. 1999. The lost "Inca-Plateau": cause of flat subduction beneath Peru? *Earth Planet. Sci. Lett.* 171:335–341.
- Haerberlin, Y. 2002. Geological and structural setting, age, and geochemistry of the orogenic gold deposits at the Pataz Province, eastern Andean Cordillera, Peru. PhD

- thesis, University of Geneva. *Terre Environ.* 36, 183 p.
- Hampel, A. 2002. The migration history of the Nazca Ridge along the Peruvian active margin: a re-evaluation. *Earth Planet. Sci. Lett.* 203:665–679.
- Haschke, M.; Scheuber, E.; Günther, A.; and Reutter, K.-J. 2002a. Evolutionary cycles during the Andean orogeny: repeated slab breakoff and flat subduction. *Terra Nova* 14:49–55.
- Haschke, M.; Siebel, W.; Günther, A.; and Scheuber, E. 2002b. Repeated crustal thickening and recycling during the Andean orogeny in north Chile (21°–26°S). *J. Geophys. Res.* 107 B1:ECV6-1–ECV6-18.
- Hildreth, W., and Moorbath, S. 1988. Crustal contributions to arc magmatism in the Andes of central Chile. *Contrib. Mineral. Petrol.* 98:455–489.
- Hollings, P.; Cooke, D. R.; and Clark, A. H. 2005. Regional geochemistry of Tertiary igneous rocks in central Chile: implications for the geodynamic environment of giant porphyry copper and epithermal gold mineralization. *Econ. Geol.* 100:887–904.
- Instituto Geológico Minero y Metalúrgico del Perú. 1995. *Geología del Perú, serie A: carta geológica nacional, boletín 55.* Lima, Inst. Geol. Min. Metal. Perú, 177 p., 5 maps.
- Jenner, G. A.; Longerich, H. P.; Jackson, S. E.; and Fryer, B. J. 1990. ICP-MS: a powerful new tool for high-precision trace element analysis in earth sciences: evidence from analysis of selected USGS standards. *Chem. Geol.* 83:133–148.
- Johnson, R. F. 1955. Geology of the Atacocha mine, department of Pasco, Peru. *Econ. Geol.* 50:249–270.
- Jurard, J.; Dipple, G.; Ebert, S. E.; and Tosdal, R. M. 2004. Distal alteration around the carbonate hosted polymetallic replacement and skarn system at Yauricocha, central Peru. XII Congreso Peruano de Geología (Lima, 2004), Proc., p. 664–665.
- Kay, S. M., and Mpodozis, C. 2001. Central Andean ore deposits linked to evolving shallow subduction systems and thickening crust. *GSA Today* 11:4–9.
- Kay, S. M.; Mpodozis, C.; and Coira, C. 1999. Neogene magmatism, tectonism and mineral deposits of the central Andes (22° to 33°S latitude). In Skinner, B. J., ed. *Geology and ore deposits of the central Andes.* Soc. Econ. Geol. Spec. Publ. 7:27–59.
- Kay, S. M.; Mpodozis, C.; Ramos, V. A.; and Munizaga, F. 1991. Magma source variations for mid-late Tertiary magmatic rocks associated with a shallowing subduction zone and a thickening crust in the central Andes (28–33°S). In Harmon, R. S., and Rapela, C., eds. *Andean magmatism and its tectonic setting.* *Geol. Soc. Am. Spec. Pap.* 265:113–137.
- Kouzmanov, K.; Bendežú, A.; Catchpole, H.; Agneau, M.; Pérez, J.; and Fontboté, L. 2008. The Miocene Morococha district, central Peru: large-scale epithermal polymetallic overprint on multiple intrusion-centered porphyry systems. Australasian Institute of Mining and Metallurgy PACRIM Congress (Queensland, 2008), Proc., p. 117–121.
- LeBas, M. J.; LeMaitre, R. W.; Streckeisen, A.; and Zannettin, B. 1986. A chemical classification of volcanic rocks based on the total alkali silica diagram. *J. Petrol.* 27:745–750.
- Love, D. A.; Clark, A. H.; and Glover, K. J. 2004. The lithologic, stratigraphic and structural setting of the giant Antamina copper-zinc skarn deposit, Ancash, Peru. *Econ. Geol.* 99:887–916.
- Love, D. A.; Clark, A. H.; and Lipten, E. J. H. 2003. Genesis of the Antamina Cu-Zn Skarn deposit, Ancash, Peru. X Congreso Geológico Chileno, Universidad de Concepción, Chile, Proc., CD-ROM.
- Macfarlane, A. W. 1999. Isotopic studies of northern Andean crustal evolution and ore metal sources. In Skinner, B. J., ed. *Geology and ore deposits of the central Andes.* Soc. Econ. Geol. Spec. Publ. 7:195–217.
- Macfarlane, A. W.; Marcet, P.; LeHuray, A. P.; and Petersen, U. 1990. Lead isotope provinces of the central Andes inferred from ores and crustal rocks. *Econ. Geol.* 85:1857–1880.
- Macfarlane, A. W.; Tosdal, R. M.; Vidal, C. E.; and Paredes, J. 1999. Geologic and isotopic constraints on the age and origin of granite-hosted auriferous-quartz veins in the Parcoy mining district, Pataz gold province, Peru. In Skinner, B. J., ed. *Geology and ore deposits of the central Andes.* Soc. Econ. Geol. Spec. Publ. 7:267–279.
- Martin, H. 1999. Adakitic magmas: modern analogues of Archaean granitoids. *Lithos* 46:411–429.
- Mégard, F. 1984. The Andean orogenic period and its major structures in central and northern Peru. *J. Geol. Soc. Lond.* 141:893–900.
- Mukasa, S. B. 1986. Lead isotopic compositions of the Lima and Arequipa segments in the coastal batholith, Peru. *Geochim. Cosmochim. Acta* 50:771–782.
- Mukasa, S. B., and Tilton, G. R. 1985. Lead isotope systematics in batholithic rocks of the western and coastal cordilleras, Peru. In Harmon, R. S., and Barreiro, B. A., eds. *Andean magmatism, chemical and isotopic constraints.* Cheshire, Shiva, p. 180–189.
- Muñoz, C. 1994. *Geologische, mineralogische und metallogenetische Untersuchungen des Jatunhuasi-Azulcocha-Chuquipita Gebietes, mit besonderer Berücksichtigung der Zn-As-(Au)-Lagerstätte Azulcocha, Zentralperu.* PhD thesis, Ruprecht-Karls-Universität, Heidelberg, 380 p.
- Noble, D. C., and McKee, E. H. 1999. The Miocene metallogenic belt of central and northern Peru. In Skinner, B. J., ed. *Geology and ore deposits of the central Andes.* Soc. Econ. Geol. Spec. Publ. 7:155–193.
- Noble, D. C.; Wise, J. M.; Vidal, C. E.; and Heizler, M. T. 1999. Age and deformational history of the “Calipuy Group” in the Cordillera Negra, northern Peru. In Benavides, V., and Rosas, S., eds. Vol. 5. 75 Aniversario Sociedad Geológica del Perú. Lima, Soc. Geol. Peru, p. 219–226.
- Peccerillo, A., and Taylor, S. R. 1976. Geochemistry of Eocene calc-alkaline volcanic rocks from the Kastamonu area, northern Turkey. *Contrib. Mineral. Petrol.* 58:63–81.
- Petersen, U.; Mayta, O.; Gamarra, L.; Vidal, C. E.; and

- Sabastizagal, A. 2004. Uchucchacua: a major silver producer in South America. *In* Sillitoe, R. H.; Perelló, J.; and Vidal, C. E., eds. *Andean metallogeny: new discoveries, concepts and updates*. Soc. Econ. Geol. Spec. Publ. 11:243–257.
- Rosenbaum, G.; Giles, D.; Saxon, M.; Betts, P. G.; Weinberg, R. F.; and Duboz, C. 2005. Subduction of the Nazca Ridge and the Inca Plateau: insights into the formation of ore deposits in Peru. *Earth Planet. Sci. Lett.* 239:18–32.
- Sajona, F. G., and Maury, R. C. 1998. Association of adakites with gold and copper mineralization in the Philippines. *C. R. Acad. Sci. Ser. II A* 326:27–34.
- Soler, P. 1991. Contribution a l'étude du magmatisme associé aux marges actives: pétrographie, géochimie et géochimie isotopique du magmatisme Cretacé a Pliocene le long d'une transversale des Andes du Perou central: implicacions géodinamiques et métallogéniques. PhD thesis, Université Pierre et Marie Curie, Paris, 832 p.
- Soler, P., and Bonhomme, M. G. 1988. Oligocene magmatic activity and associated mineralization in the polymetallic belt of central Peru. *Econ. Geol.* 83:657–663.
- Soler, P., and Rotach-Toulhoat, N. 1990. Sr-Nd isotope compositions of Cenozoic granitoids along a traverse of the central Peruvian Andes. *Geol. J.* 25:351–358.
- Stacey, J. S., and Kramers, J. D. 1975. Approximation of terrestrial lead isotope evolution by a two-stage model. *Earth Planet. Sci. Lett.* 26:207–221.
- Strusievicz, R. O.; Clark, A. H.; Lee, J. K. W.; Farrar, E.; Slauenwhite, M.; and Hodgson, C. J. 2000. Metallogenic relationships of the Huaraz, Ancash, segment of the precious-base metal sub-province of northern Peru. Geological Society of America annual meeting (Reno, NV, 2000), Proc., abstract 20428.
- Sun, S.-S., and McDonough, W. F. 1989. Chemical and isotopic systematics of oceanic basalts: implications for mantle compositions and processes. *In* Saunders, A. D., and Norry, M. J., eds. *Magmatism in the ocean basins*. Geol. Soc. Am. Spec. Publ. 42:313–345.
- Thieblemont, D.; Stein, G.; and Lescuyer, J. L. 1997. Gisements épithermaux et porphyriques: la connexion adakite. *C. R. Acad. Sci. Ser. II A* 325:103–109.
- Thouvenin, J.-M. 1983. Les minéralisations polymétalliques à Zn-Pb-Cu-Ag de Huarón, Pérou central: minéralographie des minéralisés et pétrographie des altérations de épontes. Paris, École Supérieure des Mines, 223 p.
- Tosdal, R. M., and Munizaga, F. 2003. Changing Pb sources in Mesozoic and Cenozoic Andean ore deposits, north-central Chile (30°–34°S). *Mineral. Deposit.* 38:234–250.
- Tosdal, R. M.; Wooden, J. L.; and Bouse, R. M. 1999. Pb isotopes, ore deposits, and metallogenic terranes. *In* Lambert, D. D., and Ruiz, J., eds. *Application of radiogenic isotopes to ore deposit research and exploration*. *Rev. Econ. Geol.* 12:1–28.
- Vidal, C. E., and Ligarda, R. 2004. Enargite-gold deposits at Marcapunta, Colquijirca mining district, central Peru: mineralogic and geochemical zoning in subvolcanic limestone-replacement deposits of high-sulfidation epithermal type. *In* Sillitoe, R. H.; Perelló, J.; and Vidal, C. E., eds. *Andean metallogeny, new discoveries, concepts and updates*. Soc. Econ. Geol. Spec. Publ. 11:231–241.
- Weis, D.; Kiefer, B.; Maerschalk, C.; Barling, J.; De Jong, J.; Williams, G. A.; Hanano, D.; et al. 2006. High-precision isotopic characterization of USGS reference materials by TIMS and MC-ICP-MS. *Geochem. Geophys. Geosyst.*, doi:10.1029/2006GC001283.
- Weis, D.; Kiefer, B.; Maerschalk, C.; Pretorius, W.; and Barling, J. 2005. High-precision Pb-Sr-Nd-Hf isotopic characterization of USGS BHVO-1 and BHVO-2 reference materials. *Geochem. Geophys. Geosyst.*, doi:10.1029/2004GC000852.
- Zimmerman, W. G. 1983. Investigaciones mineralógicas y petrológicas en el depósito Felicidad. *Bol. Soc. Geol. Perú* 70:51–60.

Copyright of *Journal of Geology* is the property of University of Chicago Press and its content may not be copied or emailed to multiple sites or posted to a listserv without the copyright holder's express written permission. However, users may print, download, or email articles for individual use.